Rec 28 Oct 88

(2)

AFOSR-TR- 88-1291

Final Scientific Report

AFOSR Grant No. 83-0071

February 15, 1983 to August 15, 1988

STUDIES IN THE COMPUTATION OF COMPRESSIBLE AND VISCOUS FLOW

Submitted to:

Air Force Office of Scientific Research

Submitted by:

K.-Y. Fung, Associate Professor
Department of Aerospace & Mechanical Engineering

ENGINEERING EXPERIMENT STATION
COLLEGE OF ENGINEERING AND MINES
THE UNIVERSITY OF ARIZONA
TUCSON, ARIZONA 85721

UNCLASSIFIED
SECURITY CLASSIFICATION OF THIS PAGE

ADA202334

REPORT DOCUMENTATION PAGE

1a. REPORT SECURITY CLASSIFICATION: Unclassified	1b. RESTRICTIVE MARKINGS: None
2a. SECURITY CLASSIFICATION AUTHORITY: N/A	3. DISTRIBUTION/AVAILABILITY OF REPORT: Approved for Public Release, ~~N/A~~ Distribution Unlimited
2b. DECLASSIFICATION/DOWNGRADING SCHEDULE	
4. PERFORMING ORGANIZATION REPORT NUMBER(S)	5. MONITORING ORGANIZATION REPORT NUMBER(S): N/A AFOSR-TR- 88-1291
6a. NAME OF PERFORMING ORGANIZATION: University of Arizona; 6b. OFFICE SYMBOL (If applicable)	7a. NAME OF MONITORING ORGANIZATION: AFOSR/NA
6c. ADDRESS (City, State and ZIP Code): Aerospace and Mechanical Engineering Building #16 Tucson, AZ 85721	7b. ADDRESS (City, State and ZIP Code): ~~USAF~~ Bolling AFB, Building 410 Wash. D.C. 20332
8a. NAME OF FUNDING/SPONSORING ORGANIZATION: AFOSR/NA; 8b. OFFICE SYMBOL (If applicable): NA	9. PROCUREMENT INSTRUMENT IDENTIFICATION NUMBER: AFOSR-83-0071
8c. ADDRESS (City, State and ZIP Code): Bolling Air Force Base Division of Air Force Science Bld. 410 Washington D.C. 20332-6448	10. SOURCE OF FUNDING NOS.

PROGRAM ELEMENT NO.	PROJECT NO.	TASK NO.	WORK UNIT NO.
61102F	2307	A1	

11. TITLE (Include Security Classification): Studies in the Computation of Compressible and Viscous Flow

12. PERSONAL AUTHOR(S): K.-Y. Fung

13a. TYPE OF REPORT	13b. TIME COVERED	14. DATE OF REPORT (Yr., Mo., Day)	15. PAGE COUNT
Final Scientific	FROM 2/15/83 TO 8/14/88	October 13, 1988	24

16. SUPPLEMENTARY NOTATION: N/A

17. COSATI CODES			18. SUBJECT TERMS (Continue on reverse if necessary and identify by block number)
FIELD	GROUP	SUB. GR.	
	20,04		

19. ABSTRACT (Continue on reverse if necessary and identify by block number)

The theme has been adaptive solution refinement. A novel approach called Truncation Error Injection (TEI) was introduced during the course of research. The idea behind TEI is very simple, i.e., the exact nodal value of the solution to a differential equation could be obtained on any grid and from solving a difference equation that models the differential equation if the truncation error were known. Although the TE is not known in general, it can be approximated on a local grid patch. This approach of approximating the local error due to discretization in effect decouples a problem of multiple disparate length scales into problems of single length scale so that they can be solved more efficiently on a computer than the original problem. Three types of applications have been demonstrated. In addition to solution refinement by TEI, we have shown that the decoupling of the unsteady computation from the steady one by TEI could significantly reduce the computing time and storage for flutter prediction, and that viscous effects can be computed separately and injected into the solution of an inviscid solver for viscous flow computation. Some of the advantages of this approach are: it requires very little modification to the base solver; no compatibility problems in using different grids and different solvers; readily suited for multi-processors.

20. DISTRIBUTION/AVAILABILITY OF ABSTRACT	21. ABSTRACT SECURITY CLASSIFICATION
UNCLASSIFIED/UNLIMITED ☒ SAME AS RPT. ☐ DTIC USERS ☐	~~N/A~~ Unclassified

22a. NAME OF RESPONSIBLE INDIVIDUAL	22b. TELEPHONE NUMBER (Include Area Code)	22c. OFFICE SYMBOL
Dr. James J. McMichael	(202) 767-4935	AFOSR/NA

DD FORM 1473, 83 APR — EDITION OF 1 JAN 73 IS OBSOLETE.

UNCLASSIFIED
SECURITY CLASSIFICATION OF THIS PAGE

I. SUMMARY

This final report summarizes the achievements and activities on the AFOSR Grant No. 83-0071 from February 15, 1983 to August 15, 1988.

The research under this grant has, to date, resulted in four journal publications and seven conference papers. One additional paper has been accepted for presentation at the AIAA 27th Aerospace Sciences Meeting, and another one will be submitted for presentation at the next AIAA Fluid Dynamics or CFD conference. It is anticipated that there will be two more journal publications for all the work that has been completed. Nine students have been supported fully or partially on this grant. Two graduated with a Ph.D., four with an M.S., and the other three continue to work on their dissertation topics.

The main theme, as originally proposed, has been adaptive solution refinement. A novel approach called Truncation Error Injection (TEI) was introduced during the course of research. The idea behind TEI is very simple, i.e., the exact nodal value of the solution to a differential equation could be obtained on any grid and from solving a difference equation that models the differential equation if the truncation error were known. Although the TE is not known in general, it can be approximated on a local grid patch. This approach of approximating the local error due to discretization in effect decouples a problem of multiple disparate length scales into problems of single length scale so that they can be solved more efficiently on a computer than the original problem. Three types of applications have been demonstrated. In addition to solution refinement by TEI, we have shown that the decoupling of the unsteady computation from the steady one by TEI could significantly reduce the computing time and storage for flutter prediction, and that viscous effects can be computed separately and injected into the solution of an inviscid solver for viscous flow computation. Some of the advantages of this approach are: it requires very little modification to the base solver; no compatibility problems in using different grids and different solvers; readily suited for multi-processors.

This method has also been applied to study problems related to the dynamic stalling of an airfoil. A key question in dynamic stall is when and where does the boundary layer separate? Our method enables one to resolve the details of a local flow field such

as the behavior of the boundary layer at the leading edge of the airfoil. This extension of our work will be reported in detail for a different AFOSR grant.

II SYNOPSES of JOURNAL PUBLICATIONS

Four journal publications are attached as Appendix I. The first paper, entitled "Adaptive Refinement with Truncation Error Injection," outlines the TEI methodology and demonstrates, with model problems in fluid mechanics, the versatility, efficiency and accuracy of the methodology. The second paper, entitled "Refined Numerical Solution of the Transonic Flow Past a Wedge", shows an application of TEI on one of the classical problems in transonic flows. A solution accurate to 1% of the drag value of the flow over a wedge has been obtained using TEI. An analysis of this result confirmed for the first time the existence of a weak oblique shock right after the expansion at the shoulder in addition to the normal shock downstream. The third paper, entitled "Computation of Unsteady Transonic Aerodynamics with Truncation Error Injection," extends the TEI methodology to decouple the computations of the unsteady aerodynamics due to unsteady body motion and the steady aerodynamics due to body thickness such that the unsteady computation can be done more efficiently on a much coarser grid than that used for the steady flow computation. A factor of sixteen in the saving of computing time has been demonstrated using examples of oscillating airfoil in the transonic speed range. The fourth paper, entitled "Computation with Error Injection," was an invited paper presented at the Sixth International Conference of Numerical Modelling in Science and Technology. This paper reviews the TEI methodology and further generalizes it to accommodate the use of different equations on different grids.

III PAPERS to be PUBLISHED

A paper entitled "Viscous-Inviscid Interaction and Local Grid Refinement Via Truncation Error Injection," has been accepted for presentation at the AIAA 27th Aerospace Sciences Meeting of January, 1989 in Reno, Nevada. It will be shown that accurate prediction of the flow over an airfoil can be obtained by solving the Euler equation on a relatively coarse global grid with viscous effects computed separately on a

boundary-layer type grid and injected into the global grid solution as a combination of vorticity and truncation error. In addition to the efficiency and accuracy gained by using TEI, the solution on the local grid reveals details of the shock structure and a jet-like flow emanating from the root of the normal shock in the shock boundary layer interaction zone. This result has already shed some light on the possible mechanisms causing the onset of separation of dynamic stall. It is anticipated that a further extension of the TEI methodology to equation solvers in body-fixed coordinates and nonstationary grid will allow us to explore this important area of research.

Another paper under preparation for presentation and publication is called "An Efficient Scheme for Three-Dimensional Unsteady Transonic Computations". Many techniques, including TEI, have been incorporated into an full potential code in generalized coordinates to achieve both accuracy and computational efficiency for flutter prediction for the transonic regime. A full scale application of this scheme on the prediction of the flutter boundary of an AGARD standard wing will be demonstrated.

These papers will be sent to AFOSR as soon as they have been published.

IV THESIS TITLES and AUTHORS

"Numerical Studies of Shock Wave Resolution By Mesh Refinement", Masters Report, 1984 -- J. M. Tripp

"Computations of Unsteady Transonic Aerodynamics with Truncation Error Injection", Masters Report, 1985 -- J.-K. Fu

"Refined Numerical Solutions of The Transonic Flow Past a Wedge", Ph.D. Dissertation, 1985 -- S.-M. Liang

"A Truncation Error Injection Approach to Viscous-Inviscid Interaction", Ph.D. Dissertation, 1988 -- B. D. Goble

"An Efficient Scheme for Three-Dimensional Unsteady Transonic Computations", Masters Report, 1988 -- J. G. Schoen

These reports and dissertations are available upon request.

V CONFERENCE PRESENTATIONS

"The Effects of Compressibility on Dynamic Stall" (with L. W. Carr), AIAA/ASME/SIAM/APS 1st National Fluid Dynamics Congress, July 25-28, 1988, Cincinnati, Ohio, Vol. II, pp. 799-805, Paper 88-3541-CP.

"An Analytical Study of Compressibility Effects on Dynamic Stall" (with L. W. Carr), AFOSR/FJSRL/DFAN/U. Colorado Workshop II on Unsteady Separated Flows, July 20-30, 1987.

"Efficient Computations With Error Injection" (with B. D. Goble), Invited Paper, Proc. Sixth International Conference on Mathematical Modelling, August 4-7, 1987, St. Louis, Missouri.

"A Truncation Error Injection Approach to Viscous-Inviscid Interaction" (with B. D. Goble), AIAA 25th Aerospace Science Meeting, January 12-15, 1987, Reno, Nevada, AIAA Paper 87-540.

"Refined Numerical Solutions of the Transonic Flow Past a Wedge" (with S. H. Liang), Paper No. AIAA-85-1593, presented at AIAA 18th Fluid Dynamics and Plasma Dynamics and Lasers Conference, Cincinnati, Ohio, July 1985.

"Computation of Unsteady Transonic Aerodynamics With Steady State Fixed by Truncation Error Injection" (with J.-K. Fu), Paper No. AIAA-85-1644, presented at AIAA 18th Fluid Dynamics and Plasma Dynamics and Lasers Conference, Cincinnati, Ohio, July 1985.

"A Truncation Error Injection Approach to Viscous-Inviscid Interaction" (with B. D. Goble), Session Ce: Vortex Motion I, 38th Annual APS Meeting, Tucson, Arizona, November 1985.

APPENDIX I

Journal Publications

Mathl Comput. Modelling, Vol. 11, pp. 1116–1121, 1988
Printed in Great Britain

0895-7177/88 $3.00 + 0.00
Pergamon Press plc

COMPUTATION WITH ERROR INJECTION

K.-Y. Fung and Brian D. Goble

University of Arizona, Aerospace and Mechanical Engr. Dept., Bldg. 16, Tucson, AZ 85721 USA

Abstract. In the context of computational fluid dynamics, the adaptive refinement technique with truncation error injection due to Fung et al (1984) is extended to include differences in the governing equations being used on the fine and coarse grids. This method allows the decoupling of a problem of multiple length scales into problems of simple length scale which can be more efficiently resolved on separate grids and using different formulations pertinent to the length scales than on a single grid. Three variants of this method are exemplified with applications to problems in computational fluid dynamics. Substantial savings in computer time and storage are achieved in the examples.

Keywords. Solution refinement; Truncation error; Multiple grid; Multigrid.

INTRODUCTION

In the following we will introduce a methodology which allows the decoupling of a complex problem of distinct length scales into problems of simple length scale so that they can be solved more efficiently on a computer. The examples we have chosen here to apply this methodology to are problems in computational aerodynamics, since they are of our prime interest. We hope a review of our works in the development of this methodology will make it known to other disciplines and further its applications.

Computation of flows over aerodynamic bodies has reached a stage where solutions to most engineering problems can be found with some degree of accuracy. Solvers are available for equation sets ranging from the Laplace equation for subsonic or supersonic flow to the Reynolds-averaged compressible Navier-Stokes equations for transonic flow. The choice of equations to be solved to predict some given flow situation depends on such variables as degree of accuracy required, computer resources available, codes available, complexity of geometry, and complexity of flow situation. Ideally, the most accurate code available would be used on a grid with sufficient resolution to capture all of the relevant physics of the flow field. However, the computer resources in terms of memory and CPU time required to implement the desired code on a suitable grid are always limited.

The generation of such a grid is one of the main stumbling blocks in the solution process. One way to simplify the grid generation process and to increase the resolution for a given number of points is to break up a single global grid into several local grids that either overlap each other or interact through a single, coarse, global grid. The local grids could be generated about individual components of the geometry or in regions where the characteristic length scale is much smaller than that of the global flow field, such as around the leading or trailing edge of an airfoil, in the boundary layer or around a shock. Since the individual grids are only required to resolve one or two length scales, the task of generating them is greatly simplified, allowing points to be clustered where needed without wasting them elsewhere. Also, since the grids are separate, they do not have to be solved simultaneously, only requiring information pertaining to one grid to be resident in memory at a time. Although, in general, more points will be used overall, they will be used more efficiently and will give greater accuracy for a given amount of computing effort.

It is also possible to use different solvers on the different grids. Therefore, the solver that is most appropriate to the purpose of each grid can be chosen. For example, a full-potential code could be solved on a coarse global grid while the Euler equations are solved around a shock to correctly predict the shock jumps and the Navier-Stokes equations are solved in the region near the body to resolve the viscous effects that are important there. In this way, a solver that is only as sophisticated as it needs to be can be used. This approach is similar to the singular perturbation techniques in applied mathematics.

Of course, using a multiple mesh scheme adds problems inherent to the approach. Information must be passed between the grids in such a way that the overall accuracy and stability of the scheme is not compromised in any way. Also, the bookkeeping required to keep track of the solution on several different grids is more involved and needs to be automated or it will become burdensome. There is some memory and CPU time overhead due to storing bookkeeping information and setting up the grid interaction algorithms. Another possible problem area is conservation. Most solvers used today in transonic applications are in conservative or divergence form. This form is required for the scheme to conserve such quantities as mass, momentum, and energy. In regions of the flow field where the solution is smooth, conservative form is not important, but when discontinuities such as shocks appear in the solution, conservation must be maintained in order to correctly predict their location. Even if the solvers themselves are conservative, if shocks cross a grid boundary that is not treated conservatively, the accuracy of the solution could suffer.

The method described here will interact two or more grids together in the solution of unsteady, transonic, viscous flow over an airfoil. The method

will support the use of a different solver for each grid, which will be interacted through a global coarse grid using the method proposed by Fung et al(1984). This approach treats the local grid solutions as more accurate approximations to the correct flow field than the global solution and uses them to correct the global solution. In this way, the global solution feels the effect of each local grid and serves to transmit this data to each of the other local grids. Section 2 reviews the approach due to Fung et al and Section 3 extends this approach to account for differences in operators and formulations. In Section 4, we present results from three applications of the method.

TRUNCATION ERROR AND GRID REFINEMENT

Most numerical analysis books state that a differential operation L operating on a function ϕ is related to a difference operator L_h (with the subscript h denoting the grid size), operating on ϕ by the truncation error (abbreviated TE hereafter), i.e.,

$$L\phi = L_h\phi + TE(\phi,h) \tag{1}$$

This result of a Taylor series expansion is the basis for all finite difference techniques. Ordinarily, the direct system,

$$L_h\phi_h = 0 \tag{2}$$

is solved for ϕ_h. As a consistency requirement, the TE vanishes as the step size h approaches zero, leading to the limiting solution ϕ

$$\lim_{h\to 0} \phi_h = \phi \tag{3}$$

that satisfies the differential equation

$$L\phi = 0. \tag{4}$$

Hence, it is assumed that if the TE is uniformly small, solving the discrete system Eqn. (2) will lead to a good approximate solution ϕ_h, of ϕ. However, in many problems the TE is a rapidly varying function of its arguments. The idea of conventional grid-adapting techniques is to look for or modify the distribution of grid points according to some preset criteria which will render uniformity of TE across the solution domain. Unfortunately, there is no simple way to generate a grid that minimizes the TE for a given problem and, in many cases, the process of finding the optimal grid is more complicated and time consuming than computing the solution itself.

We must remember that it is Eqn. (4) that one wants to solve, not Eqn. (2). The discrete equation that ought to be solved corresponding to solving Eqn. (4) is implied by Eqn. (1), i.e.,

$$L_h\phi_h + TE(\bar{\phi},h) = 0 \tag{5}$$

Here, we have deliberately denoted the argument function ϕ of the TE with a bar, which can be different from the solution ϕ_h. Notice that if the exact solution were available, it would satisfy Eqn. (5) exactly, with $\phi = \phi_h = \phi$. This implies that the TE can be computed exactly by applying the operator L_h to the solution, e.g.,

$$TE(\phi,h) = -L_h\phi \tag{6}$$

and that solving the system

$$L_h\phi_h = -TE(\phi,h) = L_h\phi \tag{7}$$

will yield the exact solution at nodal points. Hence, it is clear that if the goal is to improve a numerical solution, the basic grid structure need not be changed, only improved values of TE at grid points need to be provided. To emphasize this point, the base grid in the examples considered here is never changed. The strategy one would use in making tradeoffs between the base grid and approximating the TE is not discussed in this paper.

Analytically, the TE consists of all higher derivatives of the function being expanded in a Taylor series, if they exist. If more neighboring values of a function are known, higher derivatives can be computed, and hence the TE can be better approximated. A TE sequence may be defined as follows:

$$TE_{h/N} = TE(\phi_{h/N},h) = -L_h\phi_{h/N} \tag{8}$$

where the subscript h/N refers to values based on a grid of size h/N (e.g., subdividing the base grid of size h, N times). For simplicity, we may assume $\phi_{h/N}$ satisfies the equation

$$L_{h/N}\phi_{h/N} = 0 \tag{9}$$

With these definitions and the substitution of Eqn. (8) into Eqn. (6) and setting $\phi = \phi_{h/N}$, it is easy to see that $\phi_h = \phi_{h/N}$ is a solution of Eqn. (5) at coinciding nodal points (or through the use of an interpolation function).

All we have shown so far is that it is possible to obtain a refined numerical solution satisfying Eqn. (5) without changing the base grid, provided the TE is known to the same order of accuracy as the solution. The inclusion of TE into the difference equation has been suggested before. Lentini and Pereyra (1974) proposed a deferred correction procedure to compute the TE progressively. Warming and Hyett (1974) and Klopfer and McRae (1983) implemented it in forms of a modified equation. For some simple linear differential equations, even analytical expressions of the TE in terms of lower derivatives of the unknown function have been used. However, the complexity involved in the derivation of such terms and, in some, the numerical instabilities caused by the presence of certain terms has discouraged the more popular use of such schemes. Liang and Fung (1985) and Fung et al (1984) both demonstrated that the above logic significantly reduced the computation work required to achieve a refined numerical solution satisfying Eqn. (5) without significantly increasing the complexity involved.

TRUNCATION ERROR DUE TO OPERATOR DIFFERENCES

Now extend the $TE(\phi,h)$ term in the above equations to include differences between the coarse grid operator and the fine grid operator, i.e. the fine grid equations can be a higher order accuracy version of the original equations or even a different equation set entirely. For example, apply the above logic to a set of equations where the operator can be split into different parts, each part representing its own physics with its own characteristic length scales, e.g. the Navier-Stokes equations (NSE). Write the NSE in operator form as

$$L_t\phi_h + L_h^I\phi_h - \mathrm{Re}^{-1}L_h^V\phi_h = 0 \tag{10}$$

where the total operator has been split into the temporal, convective, and viscous operators. Each of these operators can be associated with different aspects of the flow field having distinct length

scales. When these equations are being solved numerically, a grid must be used which can capture all of the relevant length scales, however disparate they are. Generating such a grid which will also allow the equations to be efficiently solved can be quite difficult. As mentioned earlier, we can solve each operator on a grid which resolves its own relevant physics and use TE injection to bring the separate effects to a global grid. For the sake of example, say that the physical phenomena associated with each of the operators in Eqn. (10) have length scales which decrease from left to right and that the last operator is only important in some particular region of the flow field. Then, we can solve Eqn. (11) on a grid local to that region which has sufficient resolution to capture the relevant physics.

$$L^{I}_{hIN}\phi^{v}_{hIN} - Re^{-1}L^{V}_{hIN}\phi^{v}_{hIN} = 0 \qquad (11)$$

The influence of this solution can then be forced into the global solution via TE injection by solving

$$L^{I}_{hIM}\phi^{i}_{hIM} = L^{I}_{hIM}\phi^{v}_{hIN} \qquad (12)$$

on the global grid which is only fine enough to resolve the physics relevant to the L^{I} operator, i.e. $M < N$. If the grids used in solving Eqn. (11) and Eqn. (12) cover the same domain, then the solution of Eqn. (12) will represent the fine grid solution at the coarse grid nodes, while, if the fine grid is only a subset of the total domain, the solution of Eqn. (12) will reproduce the fine grid solution at the coarse grid nodes which lie within the fine grid region with some influence from the rest of the domain.

Now, if the temporal effects can be thought of as perturbations to a steady state, Eqn. (13) can be solved for the final solution on a grid which is only as fine as necessary to resolve the unsteady physics.

$$L_{t}\phi_{h} + L^{I}_{h}\phi_{h} = L^{I}_{h}\phi^{i}_{hIM} \qquad (13)$$

As explained in Fung et al (1987), the RHS of Eqn. (13) is an approximation to the TE resulting from a Taylor's series expansion of the differential equation that Eqn. (12) is modeling. Eqn. (13), if allowed to converge to a steady state, will reproduce the fine grid solution at the coarse grid nodes. For unsteady calculations, the RHS fixes the steady solution so that only the unsteady perturbations to this solution must be resolved.

In this section we have introduced a procedure similar to that suggested by Brandt (1980) for separating the length scales of a problem so that they can be solved more efficiently. Following are some examples which show that the injection of the TE due to differences in grids and operators is a simple but effective means of improving the accuracy and efficiency of a numerical solution.

RESULTS

The first problem was chosen to study this procedure with rotated grids aligned with discontinuities in the flow field. This is a case where the fine grid operator is merely a different form of the coarse grid operator. We solved the linear, two-dimensional convection-diffusion equation for a nominal quantity T, modeling two adjacent fluids of initially different temperatures moving at the same speed. Upwind differencing was used for the convective terms. It is well known that the artificial cross-wind diffusion due to upwind differencing is a major source of error. It causes excessive spreading of the discontinuity. Fig. 1 shows the temperature contours solved on a 60x40 base grid of step size h

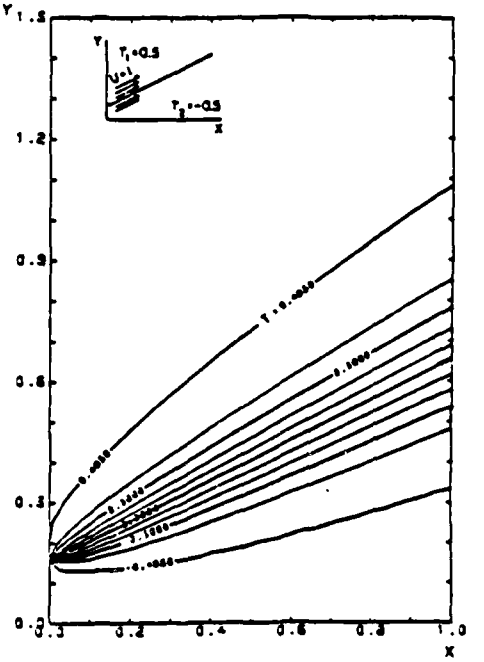

FIG. 1. Numerical Solution of a temperature diffusion layer (60x40 grid), no TE injection.

= 0.25. Solving the equations on a 120x80 grid only slightly improved the solution and neither case compared well with the exact solution. Given suitable pattern recognition schemes, it would be natural to introduce a rotated grid parallel to the flow direction over a small region surrounding the discontinuity with boundary conditions extracted from the original solution. Here, we have done this manually with a 20x40 grid aligned with the flow. Due to grid rotation, the cross-wind artificial diffusion is minimized, resulting in a sharp temperature gradient very close to the exact solution. The isotherms that appear near the upper and lower boundary of the refined local solution on the subgrid (Fig. 2) are an effect of the incorrect boundary conditions extracted from the base grid solution; these can be avoided simply by taking a larger subgrid. However, with the injected TE, the improved base solution provides a sharp gradient without such isotherms (Fig. 3), which shows that the base grid solution is readjusted smoothly through the artificial boundaries.

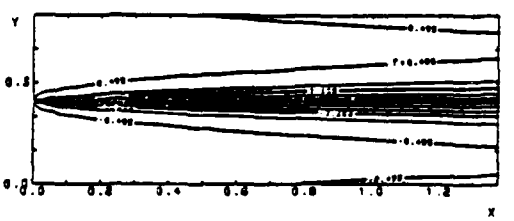

FIG. 2. Locally refined solution on a rotated 20x40 grid.

The second example is the use of TE injection to maintain the inviscid steady flow corresponding to

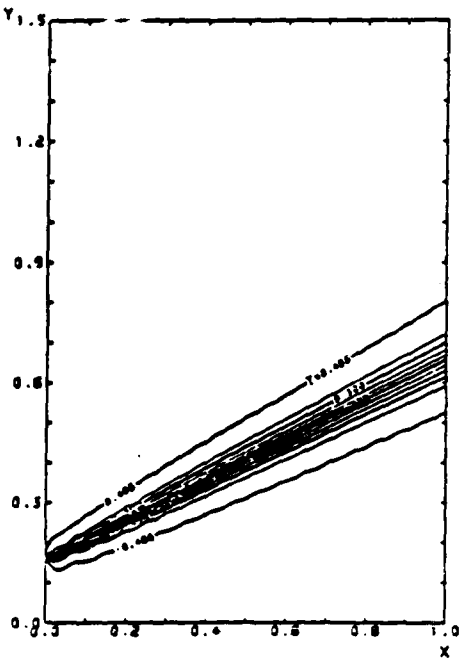

FIG. 3. Improved solution of a temperature diffusion layer with TE injection, 60x40 grid.

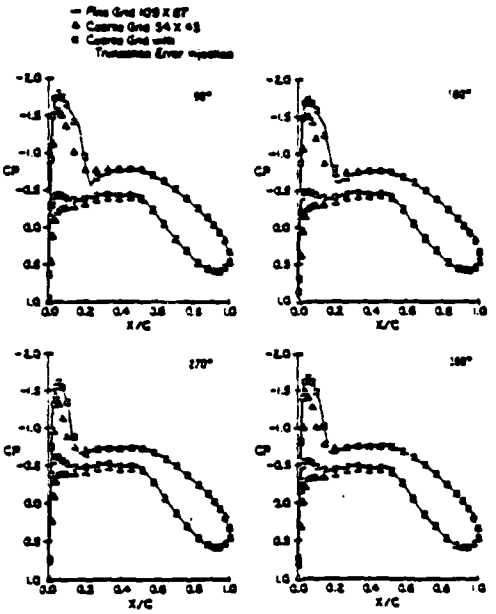

FIG. 4. Comparison of the unsteady pressure distributions of an NLR 7301 airfoil.

body shape while the perturbed unsteady flow corresponding to unsteady body motions are being computed. In unsteady transonic flow, for low to moderate reduced frequencies, the typical wave length of an acoustic signal is of the order of the chord of the wing. Hence, a grid with a minimum spacing of a tenth of the chord should be sufficiently fine to resolve these waves. However, in a typical inviscid flow, the smallest characteristic length scale is on the order of the radius of curvature of the leading edge of the airfoil. Therefore, a grid with a minimum spacing of a hundredth of a chord is needed to resolve the flow field. Due to linear or nonlinear numerical instability, these grids may require too small a time step for efficient computations of the unsteady acoustic waves caused by the small unsteady wing motions and deformation assumed in flutter analysis. In order to ease the restrictions on the time step, Fung and Fu(1985) used the technique described above to compute the steady and unsteady flows on different grids.

They assumed inviscid flow so Re→∞ and only Eqns. (12) and (13) above are relevant. Eqn. (12) is solved on a grid which is fine enough to resolve all the relevant physics in the steady flow field. Eqn. (13) is solved on a grid which is only as fine as required to resolve the acoustic signals as described above. Results are presented for supercritical flow over an NLR 7301 airfoil. The airfoil is pitching harmonically at a reduced frequency k = 0.1 in a freestream with Mach number of 0.7. The calculations were performed on a fine grid 109x87, a coarse grid 54x43, and on the coarse grid with TE injection from the fine grid. Fig. 4 compares the unsteady pressure distributions at 90 degree intervals. From these comparisons, it is evident that, except for minor differences near the shock, the results obtained on the coarse grid with TE injection are just as accurate as those on the fine grid. The fine grid solution required 900 seconds of CPU time, the coarse grid solution 57 seconds, and the coarse grid solution with TE injection 60 seconds. A reduction in computation time by a factor of four is attributed to the reduction in grid points and another factor of four to the relaxation of the allowable time step imposed by numerical stability.

This technique has also been applied by Schoen (1987) to three dimensional flow in a code developed at Nasa-Ames for Transonic UNsteady Aerodynamics - TUNA, due to Bridgeman and Steger (1982). Results are presented for supercritical flow over a rectangular wing with NACA-0012 cross-section and an aspect ratio of 6. Fig. 5 shows the deviation of the pressure coefficient from the fine grid steady state at the airfoil midspan for the fine grid solution and the coarse grid solution with TE injection. Note that the scales used in Fig. 5 do not permit us to show the large deviations found in the coarse grid solution without TE injection. The wing is plunging harmonically at a reduced frequency of 0.4 in a freestream with Mach number 0.7. The calculations were performed on a fine grid 89x49x18, on a coarse grid 45x25x18, and on the coarse grid with TE injected. The grids were not coarsened in the spanwise direction as the typical spacing in this dimension is too large on even the fine grid for resolving acoustic waves. The method captures the steady-state solution exactly. Various phases from the first cycle are shown to verify that the unsteady procedure maintains respectable accuracy as well. With 100 steps per cycle, the fine grid solution took 68 Cray seconds per cycle and the coarse grid with or without TE took 19 seconds per cycle. Because the time marching scheme in this code is unconditionally stable, there were no time step restrictions to be relaxed on the coarse grid. Thus, a reduction in computation time by a factor of about four is attributed to the reduction in grid points.

The third example shows the use of TE injection to fix the viscous effects in a steady flow field while using a less dense grid to calculate the inviscid

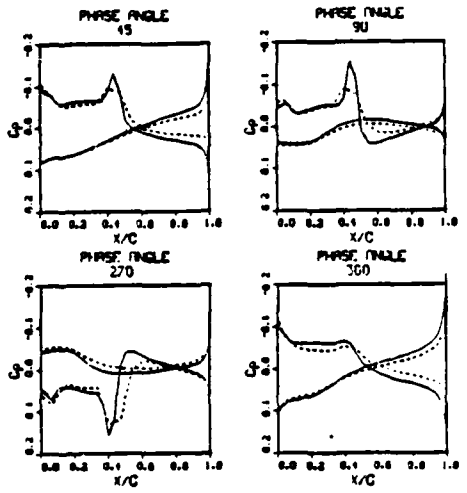

FIG. 5. Comparisons of the unsteady deviations from the fine grid steady state solution for an ONERA-M6 airfoil.

aspects of the flow. As mentioned above, a grid with a minimum spacing of a hundredth of a chord should be sufficient to resolve the inviscid flow field. However, in a viscous calculation, the important length scale is that of the boundary layer thickness which is $O(1/\sqrt{Re})$, and in a turbulent flow there is a sublayer whose length scale is even smaller. For accuracy, a grid must be used which will resolve these small scales and yet must still retain enough points away from the body to resolve the far field. These requirements, coupled with smoothness limitations, result in a highly clustered grid with a large number of nodes which tends to slow convergence of viscous calculations. In order to resolve the two regions of flow with their distinct length scales more efficiently, we have applied the above method to allow the viscous and inviscid calculations to be computed on separate grids.

The method is implemented using the thin-layer Navier-Stokes/Euler code ARC2D due to Steger (1978) and extended by Pulliam and Chaussee (1981,1984). The code was applied to a laminar, compressible boundary layer on a flat plate at zero angle of attack; see White (1974) for details of this solution.

A laminar, viscous solution was found on a 61x61 base grid, corresponding to the solution of Eqn. (11), in the full domain using ARC2D and designated the fine grid solution. At first, in Eqn. (12), the forcing terms were formed using the same grid as the coarse grid. The forced calculation was then performed with free stream initial conditions. As expected, the forced calculation returned the original solution.

Eight more grids were formed from the base grid by keeping every other or every fourth coordinate line in either direction. The fine grid solution was restricted to each of the eight coarser grids. These eight grids are subsets of the fine grid so the restriction process is merely an injection of the fine grid solution at common grid points. In each case, the forcing function was formed and a forced calculation performed using free stream initial conditions. Only the results from the finest and coarsest grids will be shown here.

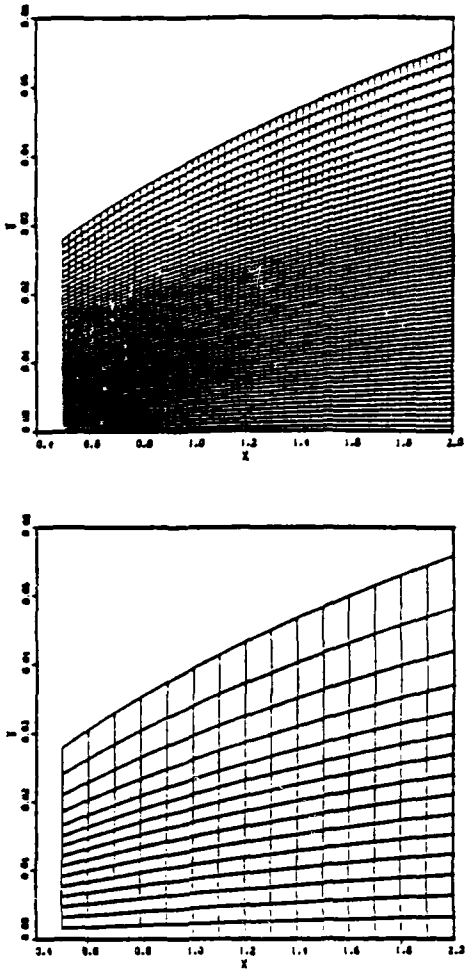

FIG. 6. Fine (61x61) and coarse (16x16) grids used for calculation of boundary layer flow.

Fig. 6 shows the two grids used. Fig. 7 compares the results found on the 16x16 grid using the Euler equations plus forcing terms (INVISJ) with the fine grid results using thin-layer Navier-Stokes (VIS4). As the plot shows, the horizontal momentum is resolved very well by the coarse grid when forcing terms are used. Fig. 7 also compares INVISJ with thin-layer Navier-Stokes results on the 16x16 grid without forcing(VISD). It is obvious that INVISJ is a far better solution than VISD.

CONCLUDING REMARKS

The technique of truncation error injection introduced by Fung et al (1987) has been successfully generalized to include operator differences in the truncation error term. This generalization has enabled the use of multiple grids to resolve widely disparate length scales, significantly increasing the efficiency of the solution process while retaining accuracy. The different grids are each required to resolve only one aspect of the flow field, making them much easier to generate and more efficient in their use of points.

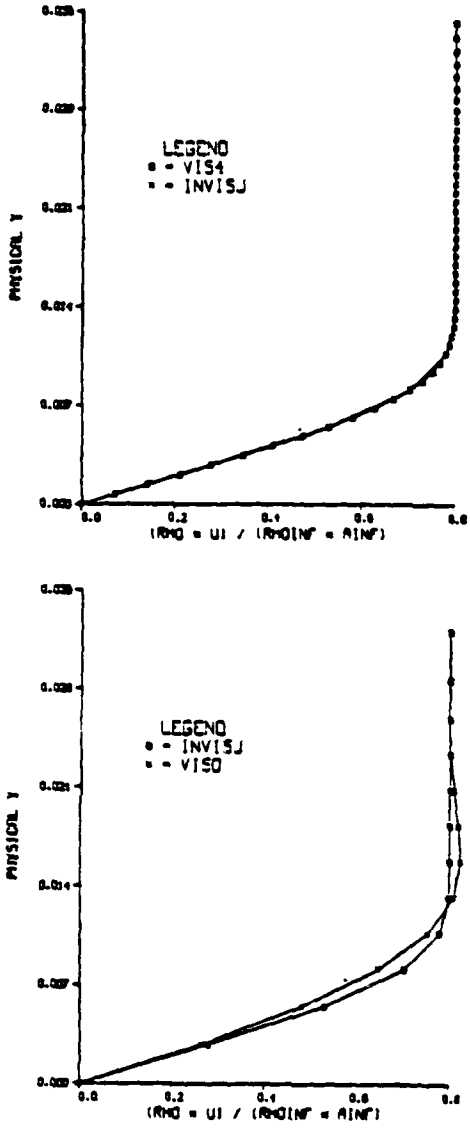

FIG. 7. Comparison of coarse grid Euler with forcing results (INVISJ) with fine grid Navier-Stokes results (VIS4), and coarse grid Navier Stokes results (VISD).

ACKNOWLEDGEMENTS

This research was carried out at the Computational Fluid Mechanics Laboratory of the Aerospace and Mechanical Engineering Department at the University of Arizona and at NASA Ames Research Center, Moffett Field, CA. The authors would like to thank NASA for support under Interchange Number NCA2-36 and the Air Force for its support under AFOSR Grant 83-0071, monitored by Dr. James D. Wilson. Permission from Dr. Terry Holst to use the NASA Ames CRAY-XMP computer for this and other studies is gratefully acknowledged. We are also thankful to Dr. Thomas Pulliam for his guidance and instruction during the second author's time at Ames.

REFERENCES

Brandt, A. (1977). Multi-Level Adaptive Solutions to Boundary Value Problems. Math. Comput. 31, 138.

Brandt, A. (1980). Multi-Level Adaptive Techniques (MLAT) for Singular-Perturbation Problems. NASA-TM-80966, N80-22016.

Bridgeman J.O. and J.L. Steger (1982). A Conservative Finite Difference Algorithm for the Unsteady Transonic Potential Equation in Generalized Coordinates. AIAA Paper 82-1388.

Fung, K.-Y., J. Tripp and B. Goble (1987). Adaptive Refinement with Truncation Error Injection. Computer Methods in Applied Mechanics and Engineering, To be published.

Fung, K.-Y. and J.-K. Fu (1987). Computation of Unsteady Transonic Aerodynamics with Truncation Error Injection. AIAA J., 25, 7.

Klopfer, G.H. and D.S. McRae (1983). Nonlinear Truncation Error Analysis of Finite Difference Schemes for the Euler Equations. AIAA J., 21, 4.

Lentini, M. and V. Pereyra (1974). A variable order finite difference method for nonlinear Multipoint Boundary Value Problems. Math. Comput. 28, 128.

Liang, S.-M. and K.-Y. Fung (1987). Refined Numerical Solution of the Transonic Flow Past a Wedge. AIAA J., 25, 9.

Pulliam, T.H. and D.S. Chaussee (1981). A Diagonal Form of an Implicit Approximate- Factorization Algorithm. J. Comput. Phys. 39, 2.

Pulliam, T.H. (1984). Euler and Thin-Layer Navier-Stokes Codes: ARC2D, and ARC3D, Notes for the Computational Fluid Dynamics Users' Workshop, University of Tennessee Space Institute, Tullahoma, Tenn.

Schoen, J.S. (1987). Master's Thesis, Dept. of Aerospace and Mechanical Engineering, University of Arizona.

Steger, J.L. (1980). Implicit Finite Difference Simulation of Flow about Arbitrary Two-Dimensional Geometries. AIAA J., 16, 7.

Warming, R.F. and B.J. Hyett (1974). The Modified Equation Approach to the Stability and Accuracy Analysis of Finite Difference Methods. J. Comput. Phys. 14, 2.

White, F.M. (1974). Viscous Fluid Flow. McGraw-Hill, New York.

Computation of Unsteady Transonic Aerodynamics with Truncation Error Injection

K.-Y. Fung and J.-K. Fu

Reprinted from
AIAA Journal
Volume 25, Number 7, July 1987, Page 1018
AMERICAN INSTITUTE OF AERONAUTICS AND ASTRONAUTICS • 1633 BROADWAY • NEW YORK, N.Y. 10019

Computation of Unsteady Transonic Aerodynamics with Truncation Error Injection

K.-Y. Fung* and J.-K. Fu†
University of Arizona, Tuscon, Arizona

Introduction

THE urgent need for effective, reliable methods for unsteady aerodynamic predictions at transonic Mach numbers is evident from the Farmer and Hanson[1] experiment in which it was observed that the flutter boundary for a wing with a supercritical cross section is substantially lower than that with a conventional one. At transonic speeds, the size and location of the embedded supersonic zone over the wing affect the way acoustic signals propagate and, hence, the aerodynamic responses to disturbances. Recent developments in computational fluid dynamics and the availability of supercomputers have made accurate flow prediction possible. However, for applications like routine flutter calculation and aircraft design optimization, the currently available codes, especially the ones for three-dimensional computations like XTRAN3S of Rizzetta and Borland[2] and USTF3 of Isogai and Suetsugu,[3] are still much too time consuming.

As mentioned in Fung,[4] one of the problems in unsteady transonic flow computation is the grid for obtaining the solution. Aside from the issue of finding the best grid for a given wing geometry, a grid must have a local mesh size comparable to the radius of curvature of the leading edge in order to properly resolve the fast expansion that determines the size of the sonic bubble and the strength and location of the shock. The computational domain must be large enough to allow the flow to relax to the freestream condition with little confinement from grid boundaries. Almost all grids currently used for aerodynamic computations are based on these considerations. However, these grids, while suitable for computing steady flows, may require (due to linear or nonlinear numerical instability) too small a time-step limitation for efficient computations of the unsteady acoustic waves due to the small unsteady wing motions and deformations assumed in flutter analysis. For low-to-moderate reduced frequencies, the typical wavelength of an acoustic signal in a transonic flow is of the order of the chord of the wing. Hence, a grid with a minimum spacing of a tenth of the chord should be sufficient. However, an accurate prediction of the steady flowfield over a wing at supercritical Mach number often requires a minimum spacing of a hundredth of the chord and, hence, a time-step requirement based on the CFL condition 10 times as restricted as that needed for accuracy.

In this Note, a technique is introduced that allows the steady and unsteady flows to be computed on different grids. To demonstrate the efficiency of this technique, the unsteady small-disturbance transonic equation is used for unsteady aerodynamic prediction. The results of applying this technique are compared to those obtained on single grids.

Computations with Truncation Error Injection

It has been shown[5] that, by solving the corresponding difference equation with the truncation error included as a forcing term, exact nodal values of the solution to a differential equation can be obtained; that if the exact solution were known, the exact truncation error can be computed at nodal points; and that the truncation error can be approximated by local grid refinement.

Consider a difference equation of the form

$$L_t\phi_h + L_h\phi_h = 0 \tag{1}$$

where L_t and L_h correspond to the temporal and spatial discrete operators, respectively, and ϕ_h the numerical solution on a grid of size h. Assuming that ϕ_h^0 is the steady-state solution of Eq. (1) satisfying

$$L_h\phi_h^0 = 0 \tag{2}$$

it is quite obvious that ϕ_h also satisfies

$$L_t\phi_h + L_h\phi_h = L_h\phi_h^0 \tag{3}$$

and that solving Eq. (3) for ϕ_h is the same as solving Eq. (1). However, Eq. (3) is more general in the sense that, if it converges, it will yield the steady state ϕ_h^0 regardless of whether ϕ_h^0 satisfies Eq. (2). For example, we could replace ϕ_h^0 by $\phi_{h/N}^0$, i.e.,

$$L_t\phi_h + L_h\phi_h = L_h\phi_{h/N}^0 \tag{4}$$

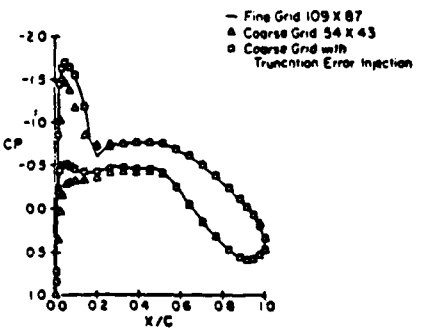

Fig. 1 Comparison of the surface pressure distributions of an NLR 7301 airfoil at $M_\infty = 0.70$ obtained by different methods on different grids.

Presented as Paper 85-1644 at the AIAA 18th Fluid Dynamics, Plasmadynamics and Lasers Conference, Cincinnati, OH, July 16-18, 1985; received Feb. 17, 1986; revision received Aug. 21, 1986.

*Associate Professor, Aerospace and Mechanical Engineering. Member AIAA.
†Research Assistant, Aerospace and Mechanical Engineering.

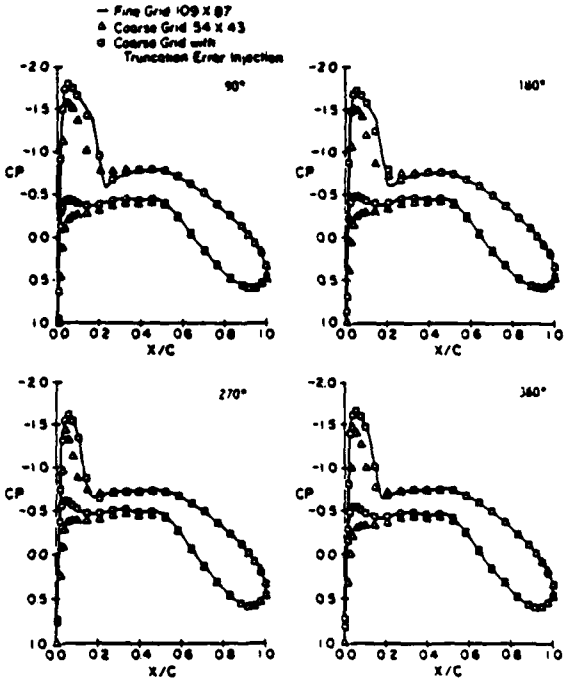

Fig. 2 Comparison of the unsteady pressure distributions (four intervals of a cycle) of an NLR 7301 airfoil pitching harmonically at $M_\infty = 0.70$ and at reduced frequency $k = 0.1$ obtained by different methods on different grids.

Table 1 Comparison of computation time for different computations, CPU's

	NACA-64A-010			NLR 7301		
Case	Steady	Unsteady	Total	Steady	Unsteady	Total
Fine grid	13.2	299.1	312.3	32.9	899.5	932.4
Coarse grid	5.5	14.5	20.0	10.4	56.5	66.9
Coarse + TEI	17.0	16.3	33.3	36.7	59.3	96.0

Here, $\phi^0_{h/N}$ denotes the steady-state solution on a finer grid of size h/N, satisfying the difference equation

$$L_{h/N}\phi^0_{h/N} = 0 \tag{5}$$

As explained in Fung et al.,[3] the term $L_h\phi^0_{h/N}$ in Eq. (4) is an approximation to the truncation error resulting from a Taylor's series expansion of the differential equation that Eq. (1) is modeling. The difference between Eqs. (3) and (4) is that the latter contains an approximation of the truncation error of the steady solution due to discretization and hence will yield the more accurate $\phi^0_{h/N}$ as a steady solution if, of course, the unsteady effects are allowed to diminish. Assuming that the base grid of size h is fine enough for resolving the unsteady part of ϕ_h, there will be very little or no truncation error due to discretization and Eq. (4) should yield more accurate solutions that Eq. (1).

In the case where the spatial operator L_h is linear, Eq. (4) is simply Eq (1) with the term $L_h\phi^0_{h/N}$ added to both sides of it. For nonlinear operators, Eq. (4) will enforce the perturbations about a steady state to satisfy the governing equation. It is of interest to note that the splitting of an operator into a steady and an unsteady operator as in Eq. (1) is necessary only for the clarity of the discussion.

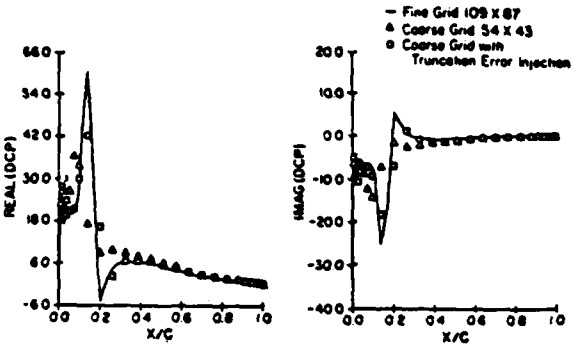

Fig. 3 Real and imaginary parts of the unsteady pressure distribution of an NLR 7301 airfoil pitching harmonically at $M_\infty = 0.70$ and at reduced frequency $k = 0.1$ obtained by different methods on different grids.

Numerical Example

To demonstrate its effectiveness, we have implemented this technique into the code AZTRAN[4] for solving the unsteady transonic small-disturbance equation. No modification to the code is needed except adding the stored truncation error values computed from the steady-state solution to the matrix equations at each time step. Figure 1 shows different steady-state pressure distributions for an NLR 7301 airfoil at a freestream Mach number $M_\infty = 0.70$ obtained on a fine grid (109×87) and on a coarse grid (54×43) that was formed by omitting every other grid line of the fine grid. As a result of faster expansion at the leading edge, the pressure distribution (solid line) obtained on the finer grid shows a stronger shock located further downstream compared to that (triangles) obtained on the coarser grid. The pressure distribution shown by the squares was obtained on the coarse grid with injected truncation error computed from the fine-grid solution. It coincides with the solid line almost everywhere except near the shock, where a smearing of the pressure jump occurs mainly because of numerical differentiation and graphic interpolation. The numerical smearing of the shock within one grid point, however, is of secondary importance as far as the computation of integrated loads for an aeroelastic application is concerned. Theoretically, unsteady perturbations on a shock create a singularity, an integrable one, however, in the perturbed quantities at the mean shock position. In reality, this singularity is often smeared by viscous effects. Motions of the shock, a nonlinear phenomenon in nature, also cause higher harmonics in the aerodynamic forces. However, it was shown by Davis and Malcolm[5] that the higher harmonics have little effect on the integrated loads.

Corresponding unsteady pressure distributions at 90-deg intervals for the same airfoil pitching harmonically at a reduced frequency $k = 0.1$ are shown in Fig. 2 and their first harmonic decompositions in Fig. 3. It is evident from these comparisons that, except for the minor differences near the shock, the results, including the motions of the shock, obtained on the coarse grid with truncation error injection are just as accurate as those on the fine grid. The CPU time, as listed in Table 1, for obtaining five cycles of harmonic motion on the fine grid was 900 s, for the coarse grid solution it was 57 s, and for the coarse grid solution with the truncation error injection it was 60 s. A reduction in computation time by a factor of four is attributed to the reduction in grid points and another factor of four to the relaxation of the allowable time step imposed by numerical stability.

Similar results for a conventional airfoil, NACA-64A-010, at a freestream Mach number of 0.796 and a reduced frequency of 0.1 are also listed in Table 1. Because of the conventional leading-edge shape, the pressure expansion at the leading edge is quite mild compared to that of the NLR 7301. Hence, the results obtained on both grids were just as accurate, except near the shock, with or without the truncation

error injection. This verifies an assumption in our theory that a relatively coarse grid is sufficient for resolving the unsteady acoustic waves if the steady pressure is accurate.

Conclusion

A simple numerical technique which can be easily implemented in any numerical code for computations of two- or three-dimensional unsteady transonic aerodynamics has been introduced. This technique allows the decoupling of a solution having two distinct length scales into two parts. By solving each part on a grid of the proper length scale, substantial savings in computation time and storage can be achieved.

Acknowledgments

This research was carried out at the Computational Fluid Mechanics Laboratory of the Aerospace and Mechanical Engineering Department under U.S. Air Force Office of Scientific Research Grant 83-0071, monitored by Dr. James D. Wilson, and NASA CFD Traineeship Grant NGT 03-002-800. Permission from Dr. Paul Kutler to use the NASA Ames Cray-XMP computer for this and other studies related to the traineeship program is gratefully acknowledged.

References

[1]Farmer, M.G. and Hanson, P.N., "Comparison of Supercritical and Conventional Wing Flutter Characteristics," *Proceedings AIAA/ASME/SAE 17th Structures, Structural Dynamics and Materials Conference*, King of Prussia, PA, April 1976, pp. 608–611 (see also NASA TMX-72837, May 1976).

[2]Rizzetta, D.P. and Borland, C.J., "Unsteady Transonic Flow Over Wings Including Viscous/Inviscid Interaction," *AIAA Journal*, Vol. 21, 1983, pp. 363–371.

[3]Isogai, K. and Suetsugu, K., "Numerical Calculation of Unsteady Transonic Potential Flow over Three-Dimensional Wings with Oscillating Control Surfaces," *AIAA Journal*, Vol. 22, April 1984, pp. 478–485.

[4]Fung, K.-Y., "A Simple, Accurate and Efficient Algorithm for Unsteady Transonic Flow," *Recent Advances in Numerical Methods in Fluid Dynamics*, edited by W.G. Habashi, Pineridge Press, Swansea, U.K., 1985.

[5]Fung, K.-Y., Tripp, J., and Goble, B., "Adaptive Refinement with Truncation Error Injection," EES Rept. CFML 84-01, University of Arizona, Tucson, 1984; also *Computer Methods in Applied Mechanics and Engineering*, to be published.

[6]Davis, S. and Malcolm, G., "Unsteady Aerodynamics of Conventional and Supercritical Airfoils," AIAA Paper 80-734, May 1980.

Refined Numerical Solution of the Transonic Flow Past a Wedge

S-M. Liang and K-Y. Fung

Reprinted from
AIAA Journal
Volume 25, Number 9, September 1987, Page 1171
AMERICAN INSTITUTE OF AERONAUTICS AND ASTRONAUTICS • 1633 BROADWAY • NEW YORK, N.Y. 10019

Refined Numerical Solution of the Transonic Flow Past a Wedge

S-M. Liang* and K-Y. Fung†
University of Arizona, Tucson, Arizona

A numerical procedure combining the ideas of solving a modified difference equation and of adaptive mesh refinement is introduced. The numerical solution on a fixed grid is improved by using better approximations of the truncation error computed from local subdomain grid refinements. This technique is used to obtain refined solutions of steady, inviscid, transonic flow past a wedge. The effects of truncation error on the pressure distribution, wave drag, sonic line, and shock position are investigated. By comparing the pressure drag to the shocks, a supersonic-to-supersonic shock originating from the wedge shoulder is confirmed.

Introduction

THE problem of interest is flow at subsonic freestream Mach number M_∞ past a wedge (see Fig. 1). After a compression at the leading edge, the flow expands and reaches the sonic condition at the shoulder. Downstream of the shoulder, the flow must return to the subsonic freestream condition through a shock, or shocks. Because of its simplicity, this model was used by Cole[1] and Yoshihara[2] to study the characteristics of transonic flow and the validity of the transonic small-disturbance equation. However, because of the inherent limitations of the hodograph method used in their studies, certain assumptions regarding the flow pattern were made in order to have a complete specification of the problem in the hodograph plane. Cole assumed that the sonic line is locally vertical and contended that the Prandtl-Meyer expansion at the wedge shoulder be terminated by an oblique shock, whereas Yoshihara assumed that a smooth overexpansion occurs at the shoulder and the supersonic zone is terminated by a normal shock downstream of the shoulder. The flow was studied experimentally by Liepmann and Bryson,[3] whose results were inconclusive about the oblique shock at the shoulder due to viscous effects, and numerically by Yu and Seebass,[4] whose solution was inaccurate due to the numerical scheme used and insufficient resolution at the shoulder. To date, no accurate solution describing the correct flow structure has been reported.

Realizing that the flow structure is a result of the expansion at the shoulder where small variations in flow variables may affect the overall flow structure, we apply a subgrid refinement procedure (suggested by Fung et al.[5]), which allows local, as well as global, improvement to obtain a refined solution on a fixed grid without changing the base grid structure, as is needed in other grid refinement procedures. In this procedure, a solution is defined on a fixed grid and is improved through approximation of the truncation error, which is usually ignored in a conventional finite-difference approximation. It is demonstrated in this study that local refinement yields results as accurate as those obtained on a uniformly refined grid, that the truncation error is an effective means for measuring error in the solution of a difference equation and for improving a numerical solution on a fixed grid, and that the procedure suggested by Fung et al.[5] achieves substantial savings in computer time and storage with minimal bookkeeping effort.

A sequence of improved solutions obtained using this method indicates the existence of both an oblique shock near the shoulder and a normal shock downstream of it.

Presented as Paper 85-1593 at the AIAA 18th Fluid Dynamics, Plasmadynamics and Lasers Conference, Cincinnati, OH, July 16-18, 1985; received March 6, 1986; revision received July 24, 1986.

*Ph.D. Candidate, Program in Applied Mathematics, Department of Mathematics; presently, Associate Professor, National Cheng-Kung University, Taiwan.

†Associate Professor, Aerospace and Mechanical Engineering. Member AIAA.

Governing Equation and Numerical Scheme

The governing equation for this flow is the transonic, small-disturbance potential equation:

$$[K\phi_x - (\phi_x^2/2)]_x + \phi_{yy} = 0 \tag{1}$$

Here, the perturbed velocity potential ϕ and the space coordinates x and y have been scaled properly. K, the transonic similarity parameter, is a result of the scaling, which involves the freestream Mach number, the wedge half thickness θ, and the ratio of specific heats γ. The boundary condition on the body is the tangency condition,

$$\phi_y(x,0) = 0, \quad x > 1$$

$$= 1, \quad 0 \le x \le 1$$

and the far-field boundary conditions are

$$\phi_x = \phi_y = 0 \text{ as } x^2 + y^2 \to \infty$$

For computational efficiency, this condition may be replaced by an analytical expression for ϕ corresponding to a source singularity at point (½, 0).

Equation (1) admits weak solutions that satisfy the shock jump condition

$$(K - \tilde{\phi}_x)[\phi_x]^2 + [\phi_y]^2 = 0 \tag{2}$$

where the tilde denotes an average quantity across the shock and the brackets denote the jump in the argument.

A balance of x momentum requires that the pressure drag on the wedge be related to the shock jumps, i.e.,

$$\int_{\text{body}} C_p \phi_y(x,0)\,dx = -\int_0^1 2\phi_x\,dx = -\frac{1}{6}\int_{\text{shocks}} [\phi_x]^3\,dy \tag{3}$$

This equation is used later for evaluating the accuracy of the results.

Equation (1) is discretized using the monotone scheme suggested by Engquist and Osher,[6] and the resultant difference equations are solved by a line relaxation method.

Truncation Error and Grid Refinement

The difference between a differential equation $\mathcal{L}\phi = 0$ and the difference equation that models it is the truncation error (denoted as TE hereafter), i.e.,

$$\mathcal{L}\phi = L_h\phi + \mathrm{TE}(\phi, h)$$

Here, $\mathcal{L}$ is the differential operator; ϕ, the solution; and L_h, the difference operator resulting from retention of appropriate leading terms in a Taylor's series expansion on a grid of typical spacing h.

Ordinarily, the discrete system, $L_h\bar{\phi}_h = 0$, is solved for an approximate $\bar{\phi}_h$ and the TE is assumed to be small. Unfortunately, unless the local grid size is comparable to, or smaller than, the local length scale of the solution, the local TE will be large, causing an error in $\bar{\phi}_h$. Attempts and limited successes have been reported on various adaptive grid distribution procedures (e.g., Pearson[7] and Babuska[8]), which tend to minimize the local TE. However, these methods very often depend on the criteria used and are sensitive to the control parameters introduced in the procedure for relating the grid sizes to the measures of error. In Ref. 5, Fung et al. explained that it should be possible to obtain at the node points of a grid the values of the exact solution to a differential equation if the TE were known. This means that if the goal is to improve the numerical solution, the basic grid structure does not have to be changed—only improved values of the TE need to be provided.

It can be shown that if the exact solution ϕ were known, the TE can be computed exactly by applying the operator L_h to ϕ, e.g.,

$$\mathrm{TE}(\phi, h) = -L_h\phi$$

Hence, *if $\phi_{h,N}$ is the refined solution on the grid of size h/N* (i.e., subdividing the base grid of size h, N times), the operation

$$-L_h\phi_{h,N} \equiv \mathrm{TE}_{h,N} = \mathrm{TE}(\phi, h)$$

would yield better approximations of the TE as the refinement factor N increases. Of course, this is true only if the scheme is consistent with the differential equation being approximated; i.e., the truncation error on the finest subgrid diminishes while the truncation error on the base grid approaches the asymptote.

To effect an improved solution on a fixed grid by TE inclusion, we use the procedure suggested by Fung et al.[5] To begin, we choose a base grid, which will not change throughout the procedure. The TE is set to zero, and the discrete equation

$$L_h\phi_h + \mathrm{TE} = 0 \tag{4}$$

is solved for the first approximation ϕ_h^0. Regarding ϕ_h^0 as a refined solution for a grid of size $2h$, an estimate of the TE is then formed by computing

$$L_{2h}\phi_h^0$$

The regions where the estimated TE, $-L_{2h}\phi_h^0$, is larger than a preset value τ are identified; if the base grid was properly chosen, these regions should be a small part of the base region. With boundary conditions interpolated from the base solution, refined solutions satisfying

$$L_{h/N}\phi_{h/N} = 0$$

are then obained and used to form the approximated TE, $-L_h\phi_{h/N}$. Outside the region where refinement is needed, the TE is assumed to remain zero. The process is repeated with the newly obtained $\mathrm{TE}_{h/N}$ until

$$|L_h\phi_{h/M}^{k+1} - L_h\phi_{h/N}^k| < \delta \text{ for all } M > N$$

This procedure is shown schematically in Fig. 2.

It was shown by Fung et al.[5] how, for various cases, this procedure can lead to improvement of numerical solution on a fixed grid, including the sharpness of shocks. A similar procedure has been suggested by Brandt.[9] He pointed out that nesting subgrids can be coupled with the multigrid procedure, which has been widely used for accelerating the convergence of numerical schemes.

Results and Discussion

The base grid for all of the numerical results is a uniform grid of spacing $h = 0.1$ over a computational domain of size 6×6 wedge chords. Figure 3 shows the distribution of the estimated TE, $L_{2h}\phi_h^0$, computed after obtaining the initial base solution ϕ_h^0. The values shown have been multiplied by a factor of 10. Subregions outside of which the maximum TE is less than the preset τ are shown in Fig. 4. No attempts were made to tailor these regions to the minimal sizes. The case of $\tau = 0$ means that the whole domain is refined. For the case of $\tau = 3.0$, two regions were identified; one is about the leading edge and the other about the shoulder, as expected. Local solutions over these regions were then obtained with interpolated boundary conditions from ϕ_h^0 (for details, see Ref. 10). From the local refined solution, the approximated truncation error is then computed and used to obtain the next refined solution, ϕ_h^1, on the base grid satisfying Eq. (4).

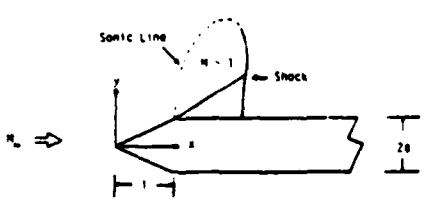

Fig. 1 Flow over a wedge at a transonic Mach number.

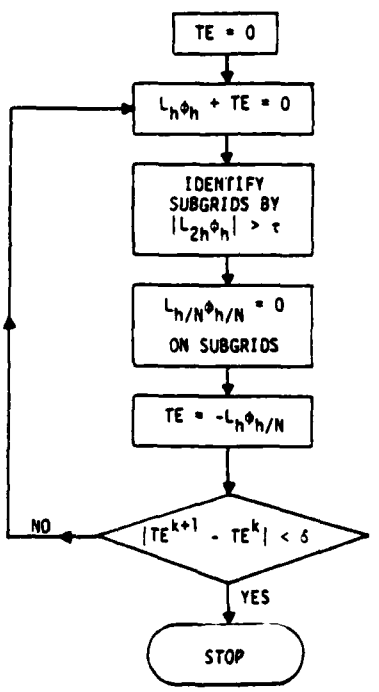

Fig. 2 Schematic of adaptive grid refinement with truncation error injection.

Table 1 Comparison of drag values for different values of τ after the first refinement cycle

Refinement cycle, k	Preset tolerance, τ	Pressure drag	Wave drag due to shocks			CPU on CRAY X-MP, s	Relative error of wave drag, %
			Oblique	Normal	Total		
0	—	0.750	0.300	0.538	0.838	33	12
1	0.00	0.772	0.201	0.610	0.811	629	5
1	0.05	0.773	0.202	0.608	0.810	66	5
1	0.50	0.770	0.179	0.627	0.806	53	5
1	3.00	0.784	0.244	0.575	0.819	50	5

Table 2 Comparison of the drag values after different cycles of refinement, $\tau = 0.05$

Refinement cycle, k	Grid refinement factor, N	Pressure drag	Wave drag due to shocks			CPU on CRAY X-MP, s	Relative error of wave drag, %
			Oblique	Normal	Total		
0	1	0.750	0.300	0.538	0.838	33	12
1	2	0.773	0.202	0.608	0.810	66	5
2	2	0.773	0.202	0.608	0.810	78	5
2	4	0.793	0.129	0.672	0.801	255	1

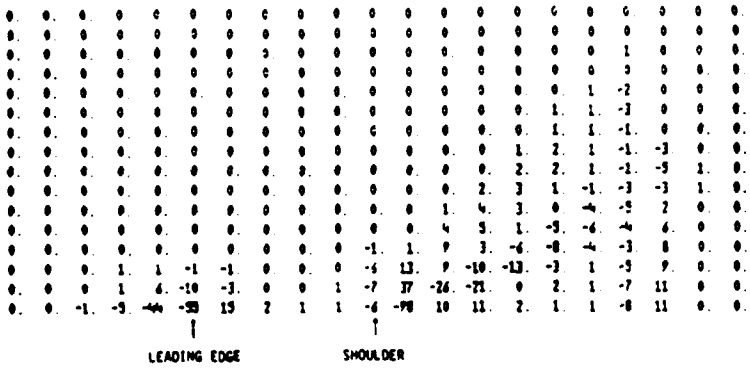

Fig. 3 Distribution of the estimated truncation error, $L_{2h}\phi_h$ (values have been multiplied by 10).

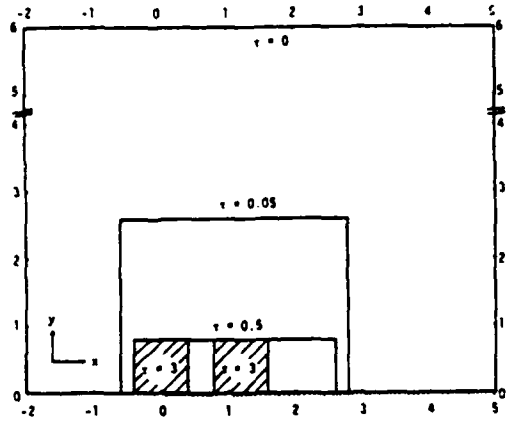

Fig. 4 Computational domain and subregions for various grid refinements.

Figure 5 compares the base solutions before and after the first cycle of refinement with that obtained on a uniformly refined grid size of $h/2$. It shows that this refinement procedure is accurate and efficient. The effects of the refinement with TE injection on the sonic line and on the shock are shown in Fig. 6. Because of the improvement at the shoulder, the normal shock moves downstream and becomes stronger. Table 1 compares values of the pressure drag on the shoulder and the wave drag due to the shocks [according to Eq. (3)] obtained for different values of τ which correspond to different regions of refinement. It is quite clear from this comparison that a subregion of $\tau = 0.05$ is adequate for accurate calculations. The difference between the wave and the pressure drag diminishes after one cycle of refinement from 12 to 5%, at a cost of only twice the computation time needed for the base solution. This is a substantial savings relative to a uniformly refined solution, which costs 20 times as much as the base grid solution ϕ_h^0. It is shown that further savings in computation time are possible with minor losses in accuracy. Another cycle of refinement, keeping the refinement factor the same ($N = 2$) but using boundary conditions from the base solution for the local refined solution, showed that the effects due to the newly updated boundary conditions on the base solution were minor compared to those of increasing N. The difference in the drag values is reduced to less than 1% after two cycles of refinement, $k = 2$, and for a refinement factor $N = 4$, but to only 5% if $N = 2$ (Table 2). For two cycles with $N = 4$, the computation time was 255 s, approximately four times that for one cycle because the total number of grid points was increased by the same factor; a better strategy would be to apply the adaptive refinement procedure to the local solution coupled with a pattern recognition routine to determine the subgrid geometry, as demonstrated by Berger and Oliger,[11] instead of the uniform refinement. The base solution obtained after two cycles of refinement was accurate within 1% in the drag values, the same order of magnitude as the maximum residual of the difference equation. Further refinements are not needed unless the residual tolerance is set to a smaller value in solving the difference equations.

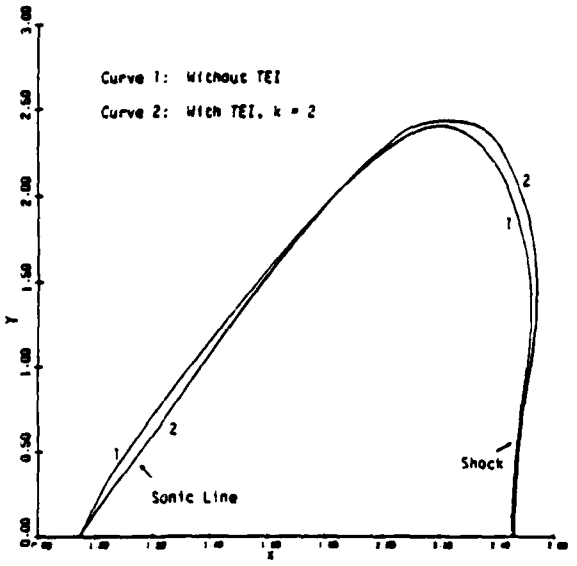

Fig. 5 Comparison of results after the first cycle of refinement, $K = 0.5$.

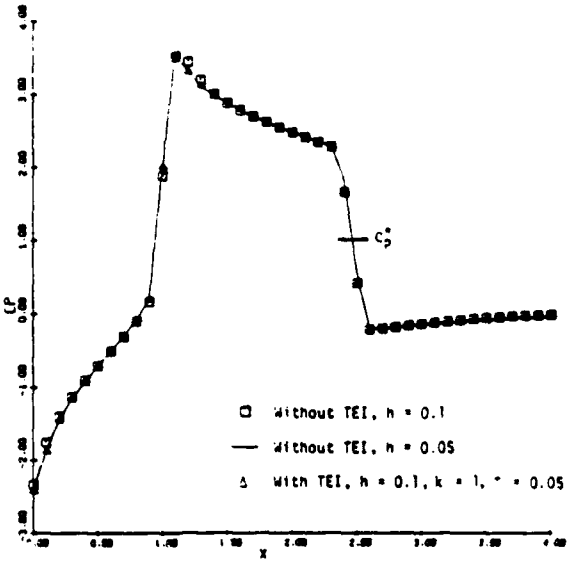

Fig. 6 Effects of truncation error injection on the sonic line and shock location, $K = 0.5$.

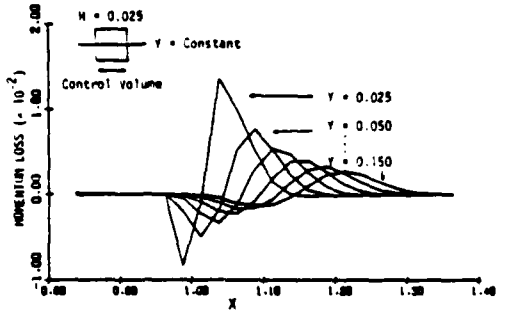

Fig. 7 Distribution of momentum losses inside a control volume at different values of y, $K = 0.5$.

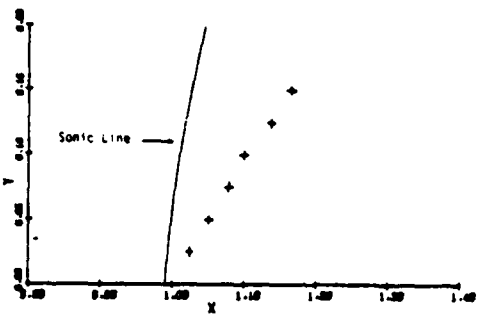

Fig. 8 Sonic line and oblique shock, $K = 0.5$.

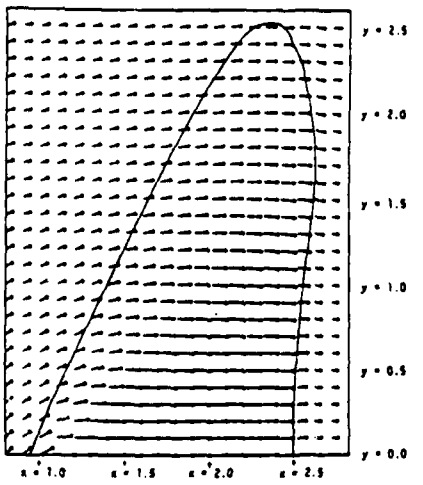

Fig. 9 Velocity field at the sonic bubble, $K = 0.5$.

In evaluating the shock drag, one notices that the drag due to the normal shock is about four-fifths of the pressure drag on the shoulder. To detect the momentum loss, we moved a control volume along a grid line parallel to the x axis and computed the losses at different x stations. These values are plotted in Fig. 7. The coordinates of the midpoint between a maximum and a minimum are shown by the crosses in Fig. 8, indicating the location of an oblique shock at an angle of about 41 deg with the x axis due to the compression immediately after the Prandtl-Meyer expansion.

A close look at the velocity field in Fig. 9 reveals the qualitative structure of the flow at the shoulder, which is of prime interest. By measuring the flow angle, it is found that the flow overexpands as much as -3.1 deg at a point 0.3 chord above and 0.6 chord downstream from the shoulder. A local analysis[12] shows that the flow expands to a maximum velocity

$$u(1^+,0) = K + (3/2)^{2/3} = 1.810$$

right after the shoulder and compresses along the wall at the rate

$$u = (3/2)^{2/3}(1 - 2^{-8/3}3x^{2/3}) + K$$

which is quite close to the numerical prediction. Because of the compression, the characteristics coalesce into a weak shock wave starting with a slope of $(2/3)^{1/3} \approx 41$ deg, a zero curvature, and a negative third derivative. The maximum velocity, linearly extrapolated from downstream to the shoulder, assumes the value 1.878 on the base grid and the

values 1.864 and 1.819 after the first and second cycles of refinement, respectively, approaching the theoretical value as the solution on the base grid is improved. It is this oblique shock that accounts for the balance of momentum.

Conclusions

An efficient refinement procedure combining the ideas of solving a modified difference equation and of adaptive mesh refinement has been developed for refined computations of steady, inviscid, transonic flows. The advantage of this procedure is that it allows local, as well as global, improvement on a base solution without changing the base grid structure and with only modest increases in storage and computation time.

In the computation of the flow over a wedge at $K=0.5$, the existence of an oblique shock near the shoulder is confirmed by comparing the pressure drag and the wave drag.

Although the present method is applied to obtain solutions of the small-disturbance equation for a particular profile, it can be extended, in principle, to other complicated flow problems.

Acknowledgments

This research was carried out in the Computational Fluid Mechanics Laboratory of the Aerospace and Mechanical Engineering Department under AFOSR Grant 83-0071, monitored by Dr. James D. Wilson, and NASA CFD Traineeship Grant NGT 03-002-800. Permission from Dr. Paul Kutler to use the NASA Ames CRAY X-MP computer for this and other studies related to the trainseeship program is gratefully acknowledged.

References

[1]Cole, J. D., "Drag of a Finite Wedge at High Subsonic Speed," *Journal of Mathematics and Physics*, Vol. 30, 1951, pp. 79–93.

[2]Yoshihara, H., "On the Flow Over a Finite Wedge in the Lower Transonic Region," WADC Tech. Rept. 56-444, ASTIA Doc. AD 110428, June 1956.

[3]Liepmann, H. W. and Bryson, A. E. Jr., "Transonic Flow Past Wedge Sections," *Journal of the Aeronautical Sciences*, Vol. 17, 1950, pp. 745–755.

[4]Yu, N. J. and Seebass, A. R., "Inviscid Transonic Flow Computations with Shock Fitting," *Symposium Transsonicum II*, edited by K. Oswatitsch and D. Rues, Springer-Verlag, New York, 1976, pp. 449–456.

[5]Fung, K-Y., Tripp, J., and Goble, B., "Adaptive Refinement with Truncation Error Injection," University of Arizona EES Rept. CRML 84-01, 1984, to appear in *Computer Methods in Applied Mechanics and Engineering*.

[6]Engquist, B. and Osher, S., "Stable and Entropy Satisfying Approximations for Transonic Flow Calculations," *Mathematics of Computation*, Vol. 34, 1980, pp. 45–75.

[7]Pearson, C. E., "On a Differential Equation of Boundary Layer Type," *Journal of Mathematics and Physics*, Vol. 47, 1968, pp. 134–154.

[8]Babuska, I., "The Self-Adaptive Approach in the Finite Element Method," *The Mathematics of Finite Elements and Applications*, Vol. II, MAFELAP, 1975, edited by J. R. Whiteman, Academic, 1976.

[9]Brandt, A., "Multi-Level Adaptive Solutions to Boundary Value Problems," *Mathematics of Computation*, Vol. 31, 1977, pp. 333–390.

[10]Liang, S-M., "Refined Numerical Solutions of the Transonic Flow Past a Wedge," Ph.D. dissertation, Univ. of Arizona, 1984.

[11]Berger, M. J. and Oliger, J., "Adaptive Mesh Refinement for Hyperbolic Partial Differential Equations," *Journal of Computational Physics*, Vol. 53, 1984, pp. 484–512.

[12]Sobieczky, H., "Transonic Wedge Shoulder Flow Singularity," Univ. of Arizona Rept. CFML 85-04, 1985.

COMPUTER METHODS IN APPLIED MECHANICS AND ENGINEERING 66 (1987) 1–16
NORTH-HOLLAND

ADAPTIVE REFINEMENT WITH TRUNCATION ERROR INJECTION

K.-Y. FUNG, John TRIPP and Brian GOBLE
Aerospace and Mechanical Engineering Department, University of Arizona, Tucson, AZ 85721, U.S.A.

Received 15 February 1985
Revised manuscript received 2 December 1986

In the context of finite difference approximation, the difference between a differential equation and the discrete (difference) equation that models it is the truncation error, and it can be easily shown that if the truncation error were known, solving the discrete equation would yield the exact solution at nodal points. An adaptive procedure for improving the accuracy of a numerical solution on a fixed grid, which we call the base, through the approximation of the truncation error by subdomain grid refinements is introduced. Regions where refinements are needed are identified using an estimate of the truncation error. Local solutions on grids tailored to each of the regions are constructed and used to form approximations to the truncation error, which is then 'injected' into the base grid to improve the base solution. A one-dimensional model of the convection-diffusion equation is used to demonstrate the basic ideas behind this method; two other examples which imply extensions of this method to multidimensional problems are also studied.

1. Introduction

Since the advent of the computer, scientists and engineers have been using discrete approximations to obtain solutions to differential equations of various complexities. Most problems can be solved using a computer, given enough storage and computation time. In practice, the class of problems that can be solved is directly limited by the available memory capacity and speed and, indirectly, by the efficiency of the method used to calculate the solution. In this paper, we introduce a grid-refinement procedure which should substantially improve the efficiency of obtaining uniformly accurate numerical solutions.

In solving a differential equation that models a physical problem of interest, e.g., the Navier–Stokes equations in fluid mechanics, the solution is represented by values at points distributed over the space on which the problem is defined. This distribution of grid points is usually at one's discretion and is generally related to the geometry and some characteristic features of the problem. It directly affects the accuracy of the solution. The optional distribution of grid points for various problems has been attempted by many researchers. A review by Thacker [1] surveyed the various methods currently used to generate grids that are geometry related. These methods are concerned with the regularity and smoothness of the

distribution of the grid generated and the satisfaction of certain predetermined criteria that are believed to be essential for accurate solutions. However, there is no guarantee that the solution obtained with such grids will meet certain accuracy requirements, nor that the number of grid points will be optimum for a given accuracy; such goals can only be realized by grids that are, at least to some degree, solution dependent.

As pointed out in a recent paper by Benek, Steger and Dougherty [2], solution-dependent grid-generation methods can be classified into three categories: grid patching, grid embedding, and grid adapting. The applications of these methods are problem oriented. Grid patching and grid embedding are based on the idea of dividing the problem domain into subdomains which are easier to handle or over which the solutions can be obtained more efficiently than over the full problem. A typical example is the aircraft design and analysis problem [3, 4]. Grid-to-grid communication is handled by interpolations, and care must be taken at intergrid boundaries to ensure certain compatibility conditions are satisfied, e.g., conservation of fluxes [5]. Usually, this type of grid generation is only problem dependent, designed according to the user's view of the problem, but can be made flexible enough to move around the problem domain, change size and density, and retire if no longer needed [6]. These procedures require extensive bookkeeping for both the grid system and the solution.

There are two grid-adapting strategies. One strategy is to redistribute a fixed number of grid points according to some criteria such that the overall error measured by some means is reduced (e.g., [7, 8]). The other is to increase the number of grid points near regions where a measure of error indicates refinement is needed (e.g., [9, 10]). These methods are most effective for problems with local singularities or layers of rapid changes, e.g., shock and boundary layers. However, a successful application of these methods depends on the criteria used for grid redistribution or addition, which may be very sensitive to the behavior of the solution, and repeated computations are needed before a satisfactory result is achieved. In the case of grid addition, redistribution of grid points may also be needed to avoid the error due to abrupt changes of grid-point distribution. For multidimensional problems, the extra effort needed to manage the complexities associated with adaptive gridding could upset the overall effectiveness of these methods. Advanced computer science techniques like pattern recognition, artificial intelligence, and data base management will definitely play a significant role in reducing the total cost of obtaining a numerical solution.

A natural question arises in refining numerical solutions: is it necessary to increase the number of grid points or redistribute them in order to improve the accuracy of a numerical solution? The answer is not as straightforward as one might think. Customarily, the error of a numerical solution is related to the truncation error or the residual due to discretization. When a measure of the truncation error is larger than a preset value in certain regions, the addition of sufficient grid points in those regions reduces the truncation error and, hence, improves the accuracy of the solution, a consistency requirement. However, it will be shown in Section 2 that an improved solution is possible without changing the base grid structure by using an approximation of the truncation error obtained from a local refinement. These two approaches, while similar in nature, are different in methodology.

An adaptive refinement procedure for solving differential equations is introduced in Section 3. Applications of this procedure to typical problems in fluid mechanics are demonstrated in Section 4.

2. Truncation error and grid refinement

Most numerical analysis books state that a differential operation L operating on a function φ is related to a difference operator L_h (with the subscript h denoting the grid size), operating on φ by the truncation error (abbreviated TE hereafter), i.e.,

$$L\varphi = L_h\varphi + TE(\varphi, h) . \tag{1}$$

This result of a Taylor-series expansion is the basis for all finite difference techniques. Ordinarily, the direct system,

$$L_h\varphi_h = 0 , \tag{2}$$

is solved for φ_h, which satisfies, consequently, the equation

$$L\varphi_h = TE(\varphi_h, h) . \tag{3}$$

As a consistency requirement, the TE vanishes as the step size h approaches zero, leading to the limiting solution φ,

$$\lim_{h\to 0} \varphi_h = \varphi ,$$

that satisfies the differential equation

$$L\varphi = 0 . \tag{4}$$

Hence, it is assumed that if the TE is uniformly small, solving the discrete system (2) will lead to a good approximate solution φ_h of φ. However, in many problems the TE is a rapidly varying function of its arguments. The idea of conventional grid-adapting techniques is to look for or modify the distribution of grid points according to some preset criteria which will render uniformity of truncation error across the solution domain. Unfortunately, there is no simple way to generate a grid that minimizes the truncation error for a given problem and, in many cases, the process of finding the optimal grid is more complicated and time consuming than computing the solution itself.

We must remember that it is (4) that one wants to solve, not (3), which is equivalent to solving the discrete equation (2). The discrete equation that ought to be solved corresponding to solving (4) is implied by (1), i.e.,

$$L_h\varphi_h + TE(\tilde{\varphi}, h) = 0 . \tag{5}$$

Here, we have deliberately denoted the argument function φ of the TE with a tilde, which can be different from the solution φ_h. Notice that if the exact solution were available, it would satisfy (5) exactly, with $\varphi = \varphi_h = \tilde{\varphi}$. This implies that the TE can be computed exactly by applying the operator L_h to the solution, e.g.,

$$\mathrm{TE}(\varphi, h) = -\mathrm{L}_h \varphi \,, \tag{6}$$

and that solving the system

$$\mathrm{L}_h \varphi_h = -\mathrm{TE}(\varphi, h) = \mathrm{L}_h \varphi$$

will yield the exact solution at nodal points. Hence, it is clear that if the goal is to improve a numerical solution, the basic grid structure need not be changed, only improved values of TE at grid points need to be provided. To emphasize this point, the base grid in the examples considered here is never changed. The strategy one would use in making tradeoffs between the base grid and approximating the TE is not discussed in this paper.

Analytically, the TE consists of all higher derivatives of the function being expanded in a Taylor series, if they exist. If more neighboring values of a function are known, higher derivatives can be computed, and hence the TE can be better approximated. A TE sequence may be defined as follows:

$$\mathrm{TE}_{h/N} = \mathrm{TE}(\varphi_{h/N}, h) = -\mathrm{L}_h \varphi_{h/N} \,, \tag{7}$$

where the subscript h/N refers to values based on a grid of size h/N (e.g., subdividing the base grid of size h, N times). For simplicity, we may assume $\varphi_{h/N}$ satisfies the equation

$$\mathrm{L}_{h/N} \varphi_{h/N} = 0 \,. \tag{8}$$

With these definitions and the substitution of (7) into (6) and setting $\tilde{\varphi} = \varphi_{h/N}$, it is easy to see that $\varphi_h = \varphi_{h/N}$ is a solution of (5) at coinciding nodal points (or through the use of an interpolation function).

All we have shown so far is that it is possible to obtain a refined numerical solution satisfying (5) without changing the base grid, provided the TE is known to the same order of accuracy as the solution. The inclusion of TE into the difference equation had been suggested before [11–14]. Pereyra [11] proposed a deferred correction procedure to compute the TE progressively. Warming and Hyett [12] and Klopfer and McRae [13] implemented it in forms of a modified equation. For some simple linear differential equations, even analytical expressions of the truncation error in terms of lower derivatives of the unknown function have been used. However, the complexity involved in the derivation of such terms and, in some cases, the numerical instabilities caused by the presence of certain terms has discouraged the more popular use of such schemes. In the following sections we will introduce an adaptive procedure similar to that suggested by Brandt [14] for solution refinements based on the ideas discussed in this section and show that the injection of the TE is a simple but effective means of improving the accuracy of a numerical solution.

3. A refinement procedure

Boundary and internal layers are common structures in nonlinear mechanics. Analytically, such layers are commonly found through singular perturbations, whereby solutions in different

regions are described by simplifed versions of the governing equation obtained using a scaling pertinent to the local features. The grid refinement procedure used here is, in many ways, analogous to the singular perturbation method. Clustering grid points over areas where rapid changes occur is effectively scaling the local solutions. A discrete operator L_h can be regarded as a simplified operator of the full equation and is valid everywhere except in regions where the omitted higher-order terms, $TE(\bar{\varphi}, h)$, become dominant.

The refinement procedure we have chosen uses the TE as an indicator and as a means for improving the solution. To begin, a base grid of size h, not necessarily uniform, is chosen for the base solution φ_h. The TE is initially assumed to be zero. Equation (5) is then solved for φ_h to a preset accuracy ε. Regarding φ_h as a refined solution for the grid $2h$, which is formed by omitting every other grid point of the base grid, the truncation error is then estimated using the formula $L_{2h}\varphi_h$ for every point of the grid h except for the boundary points and the ones next to them. The regions where the estimated TE, $-L_{2h}\varphi_h$, is larger than a preset value ε (or other appropriate criterion) are identified; for this, a pattern recognition algorithm like that described in [6] will be very useful. Outside the region where the truncation error is injected, TE is set to zero. Buffer zones are then introduced with TE = 0 but with the mesh refined to achieve smooth transition of solutions. Information on the size of the region with TE injections, solution boundary values, and parameters like the refinement factor N of these regions are then transmitted to the finer grid solver, $L_{h/N}\varphi_{h/N} = 0$, to obtain a refined local solution, $\varphi_{h/N}$. These local refined solutions are then used to form the approximated TE, $-L_h\varphi_{h/N}$, for the next cycle of refinement until

$$|L_h\varphi_{h/N} - L_h\varphi_{h/M}| < \varepsilon \quad \text{for all } M > N.$$

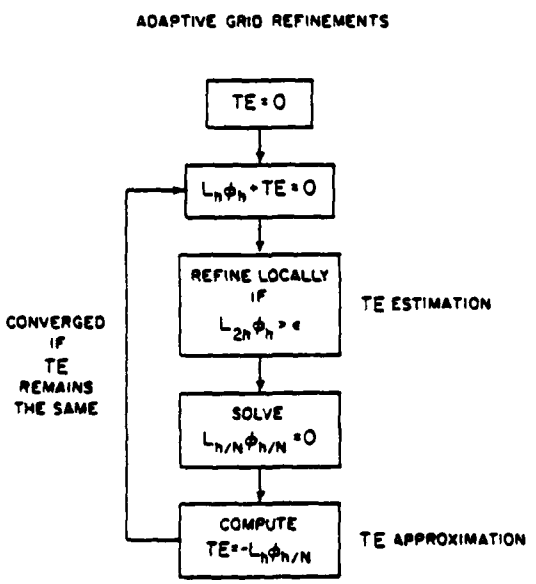

Fig. 1. Procedure for adaptive grid refinement with truncation error injection.

At this stage, further refinements will have no effect on the solution φ_h which then satisfies (5) to the preset accuracy ε. This procedure is shown schematically in Fig. 1.

Note that each refinement may have its own local solutions injecting their TE either to their parent solutions or to the base solution, its own governing equations, and its own grid distribution. No attempt is made here to optimize the strategy for grid nesting. In the case of using a local stretched grid, interpolation is needed to obtain the TE. A major advantage of truncation error injection is that, unlike other grid-refinement methods, there is no particular need for storing the finer-grid solutions. Once the TE is obtained, the approximated values of the TE indicate how good the local solution is and if needed refinements can be obtained with minor effort.

4. Numerical examples

The first example chosen to demonstrate the adaptive procedure was the classical example in boundary layer theory modeled by the one-dimensional convection-diffusion equation:

$$\varphi_x = \frac{h}{\mathrm{Re}}\,\varphi_{xx}\,, \quad \text{with } \varphi(0) = 0 \text{ and } \varphi(1) = 1\,.$$

This example has been used by many authors to demonstrate special properties of their methods.

In particular, we chose central differences for both the first and second derivatives. It is well

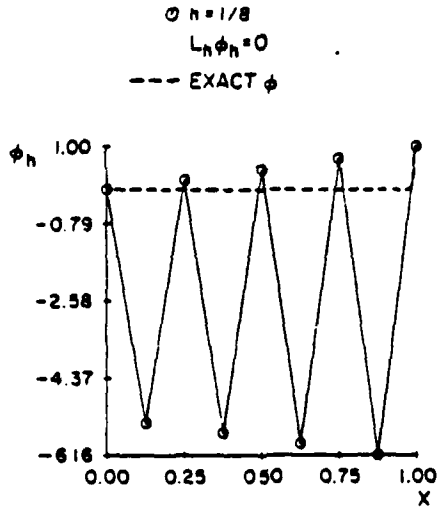

REYNOLDS NUMBER = 100
CENTRAL DIFFERENCE SCHEME
SOLUTIONS OF $hX/RE \cdot D^2\phi/DX^2 - D\phi/DX = 0$

Fig. 2. Solution without TE injection.

known that for a grid Reynolds number Re > 2, nonphysical spatial oscillations due to large dispersive truncation error occur. Figure 2 shows the erratic solution for Re = 100 and step size $h = \frac{1}{8}$. It bears no resemblance to the exact solution, which remains flat until near the right boundary and shoots up exponentially to the boundary value $\varphi(1) = 1$.

After a TE estimation (dashed line in Fig. 3(a)) which indicates that refinement is needed everywhere, the chosen subdomain (same as the base grid) is divided so it has a local step size of $\frac{1}{2}h$. A refined soution $\varphi_{h/2}$ is then obtained, solving (8), and the corresponding $TE_{h/2}$ is computed and injected into (5). The solution obtained and absolute error are depicted in Figs. 3(b), (c). The effects of the truncation error are evident by the disappearance of the nonphysical oscillations in the recomputed solution φ_h. Progressive improvements of the solution after the second and third cycle of refinement can be seen in Figs. 4 and 5. Because of the preset tolerance ($\varepsilon = 10^{-5}$), the refined region was the whole region for the above cases. Figure 6 shows a converged solution accurate within 10^{-5} in absolute error after the fourth refinement cycle. From the estimated TE, the algorithm decided that it was sufficient to refine the grid from $x = 0.375$ to $x = 1$. The total number of grid points used in the last case was 81, only a few points more than the previous refinement. It is interesting to note that in the converged solution the error is uniformly distributed across the solution domain. Further refinements showed no further improvement in the solution, indicating that the last local refinement was enough to satisfy the preset error criterion. Since this is a linear problem, a directed computation using 217 uniformly distributed points, the same total number of points used in this procedure, shows a total mean-squared error of 0.023; an improvement of 10^{-3} is achieved using this refinement strategy with the same amount of computational resources.

It is of interest to note that the choice of a scheme is immaterial to the effectiveness of this solution refinement method. We have applied it to the same problem using an upwind scheme.

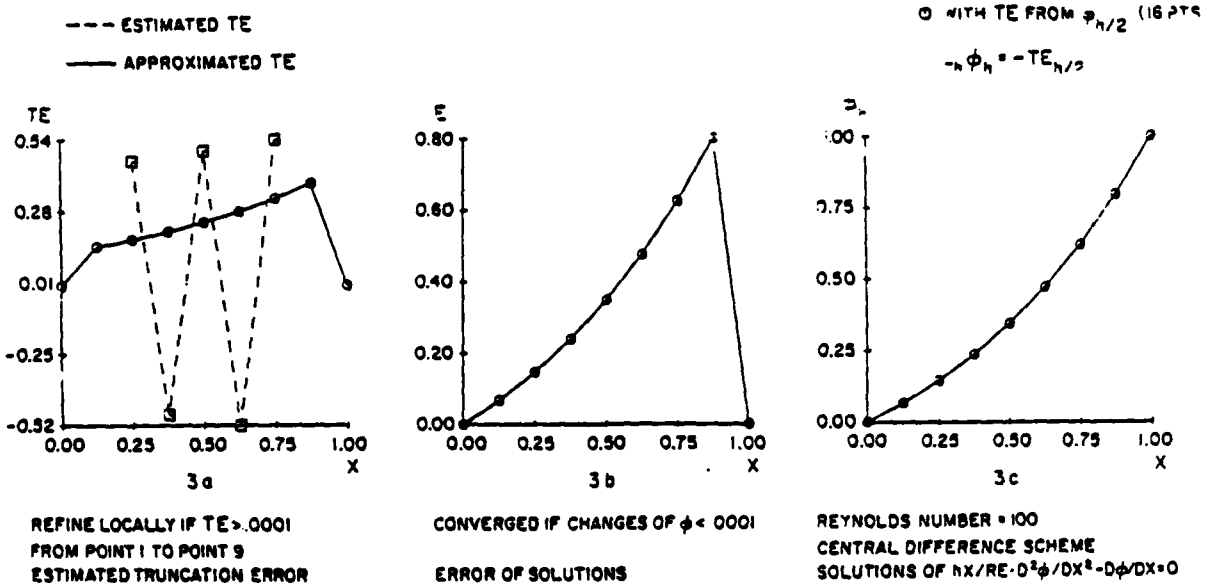

Fig. 3. Solution with TE injection after first cycle.

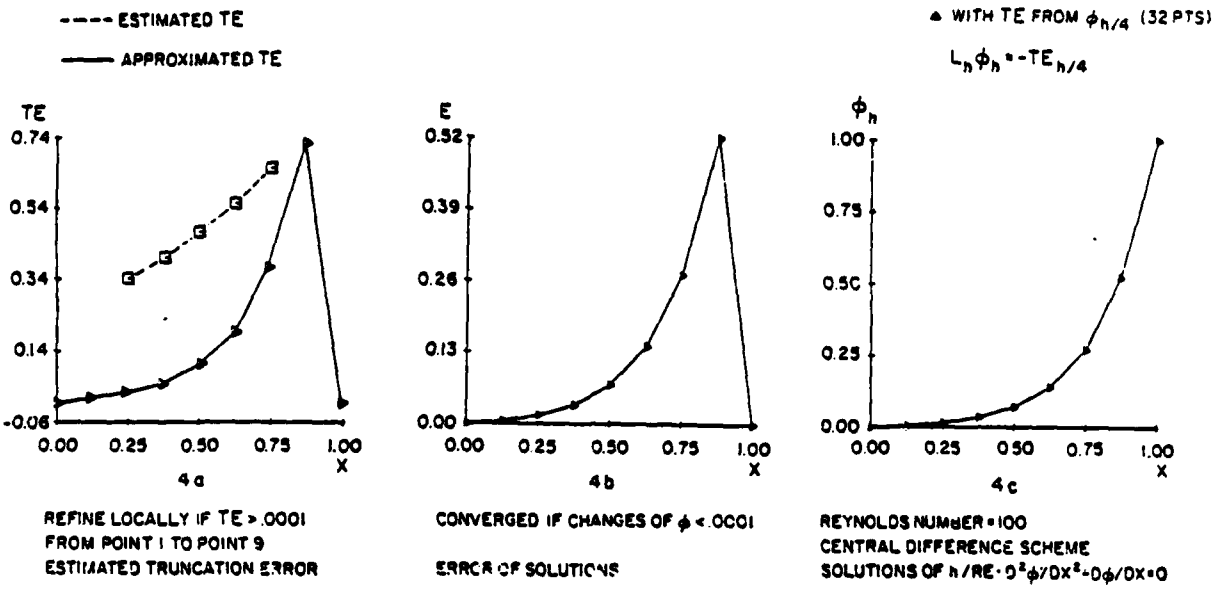

Fig. 4. Solution with TE injection after the second cycle.

The results are even more impressive. A solution accurate to 10^{-6} is achieved with two levels of local refinement and a total effort equivalent to that of using 29 points. However, the examples using central differences are more illustrative.

The second example was the reflections of a two-dimensional oblique shock from a wall. We solve the Euler's equation using the MacCormack's scheme because of its simplicity and popularity. Figure 7 shows a display of the exact pressure distribution for an incident shock, a

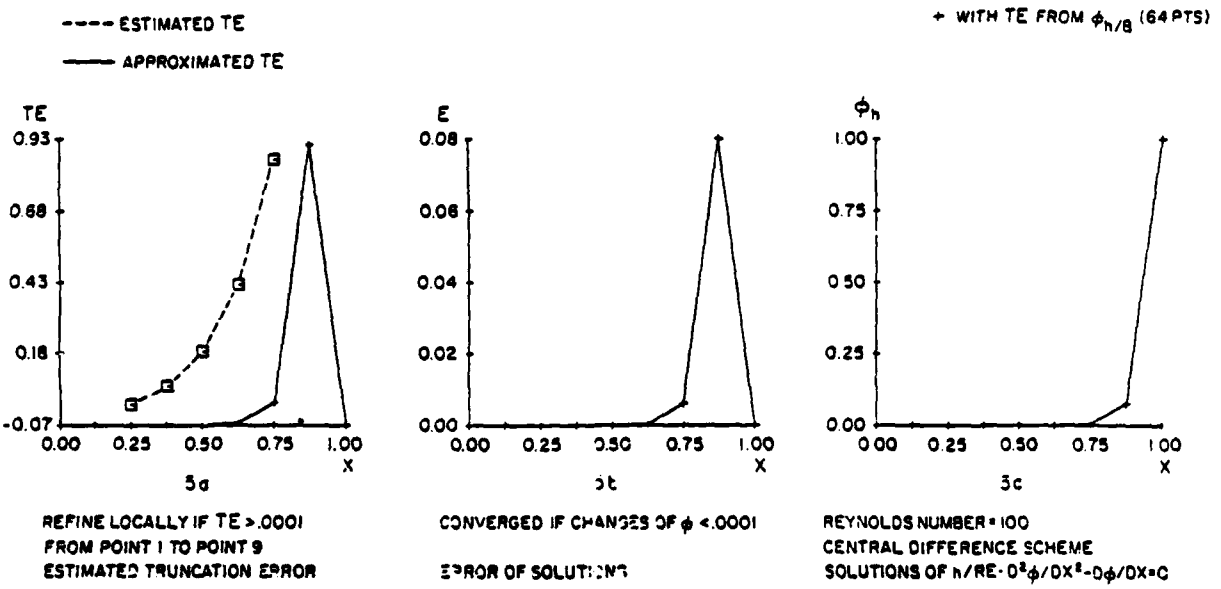

Fig. 5. Solution with TE injection after the third cycle.

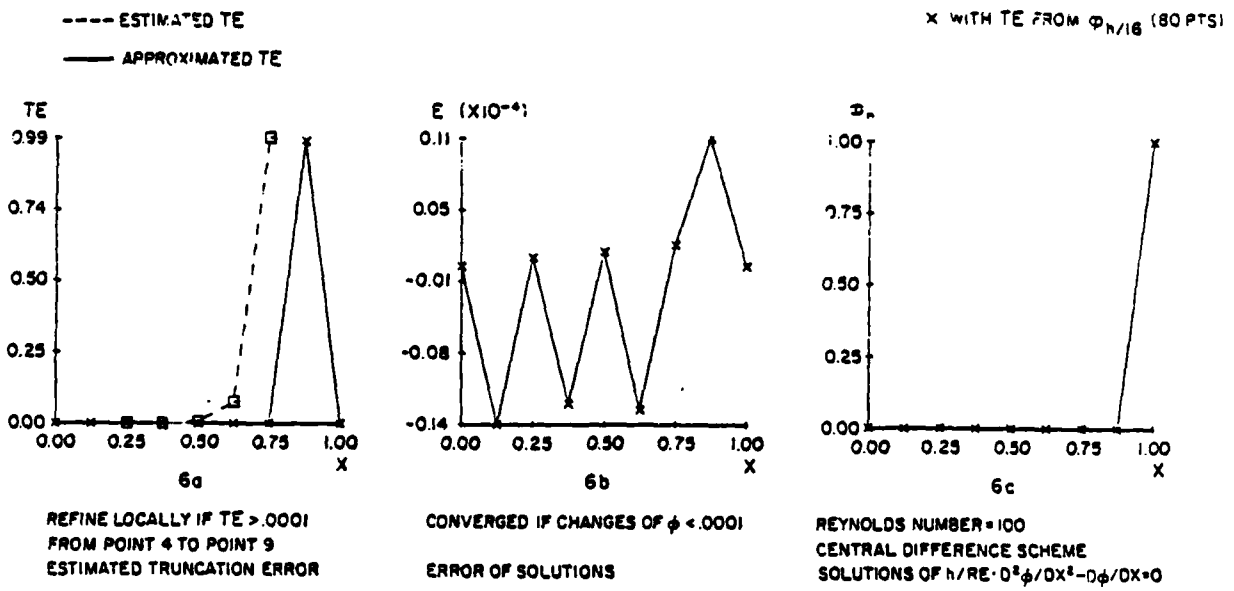

Fig. 6. Final converged solution after the fourth cycle.

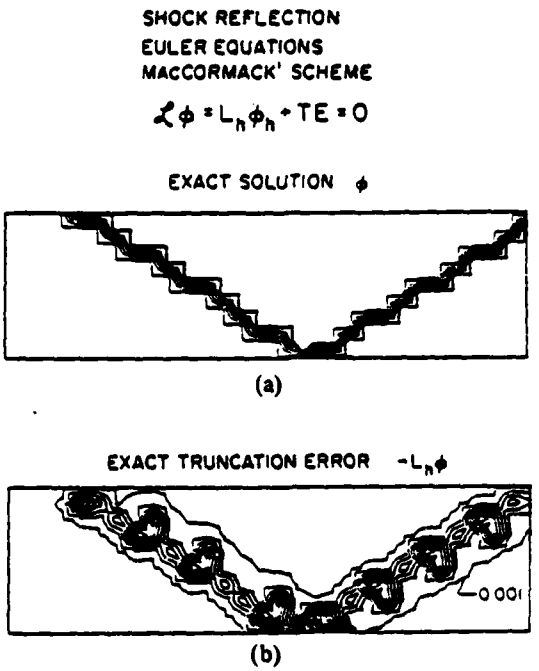

Fig. 7(a). Pressure contours of an oblique shock reflection. (b) Exact truncation error computed. TE values have an increment value of 0.001, starting at a base value of 0.01.

pressure discontinuity of 35° at free stream Mach number $M_\infty = 2.013$ over a 11×31 grid of step size $h = 0.05$. Fifteen contour levels are plotted in increments of 0.5 beginning at 0.73. The zigzags are a result of representing on a grid the abrupt pressure jump from one nodal point to another, depending on whether the point is before or after the shock, by interpolated contours for graphic display. For reference, the exact truncation error computed from the exact solution (Fig. 7(a)) is shown in Fig. 7(b) in increments of 0.005 starting at 0.001. It is clear from Fig. 7 that local refinements with rotated grids aligned with the shock would be most effective. However, our intention in this example was to show that even for a nonlinear operator, the exact solution can be recovered if the TE is given or computed locally. Figure 8 shows the approximated truncation error from a refined solution with a refinement factor of four. A comparison of the pressure contours before and after TE injection shows marked improvement. Except for the small wake behind the shocks, which is due to the numerical scheme selected, the refined solution is very close to the exact one.

The third problem was chosen to study this procedure with rotated grids aligned with the discontinuities. We solved the linear, two-dimensional convection-diffusion equation for a nominal quantity T, modeling two adjacent fluids of initially different temperatures moving at the same speed. Upwind differencing was used for the convective terms. It is well known that the artificial cross-wind diffusion due to upwind differencing is a major source of error. It causes excessive spreading of the discontinuity. Figure 9 shows the temperature contours

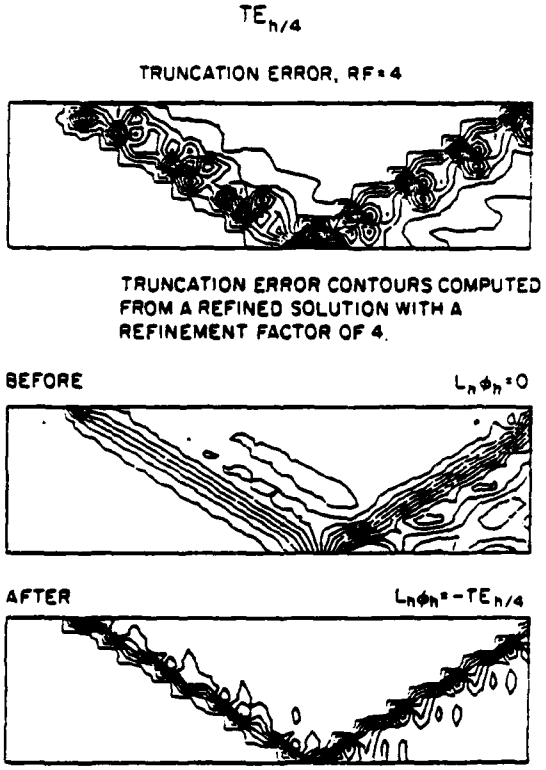

Fig. 8. Pressure contours before and after truncation error injection, $N = 4$.

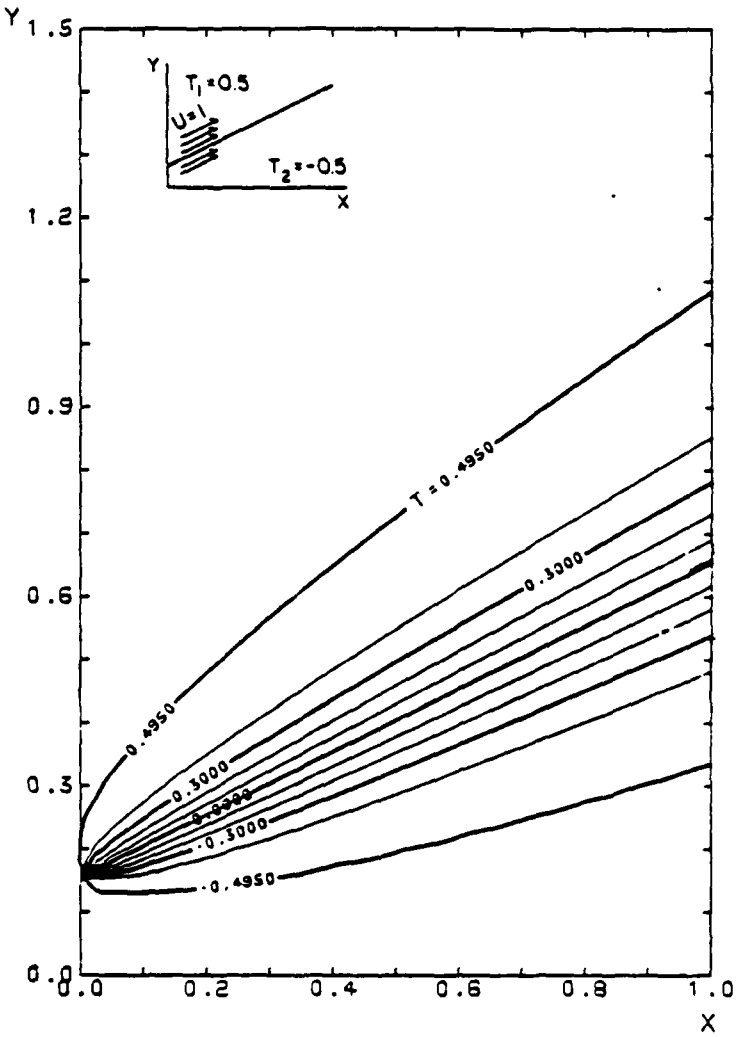

Fig. 9. Numerical solution of a temperature shear layer (grid 60 × 40), no TE injection.

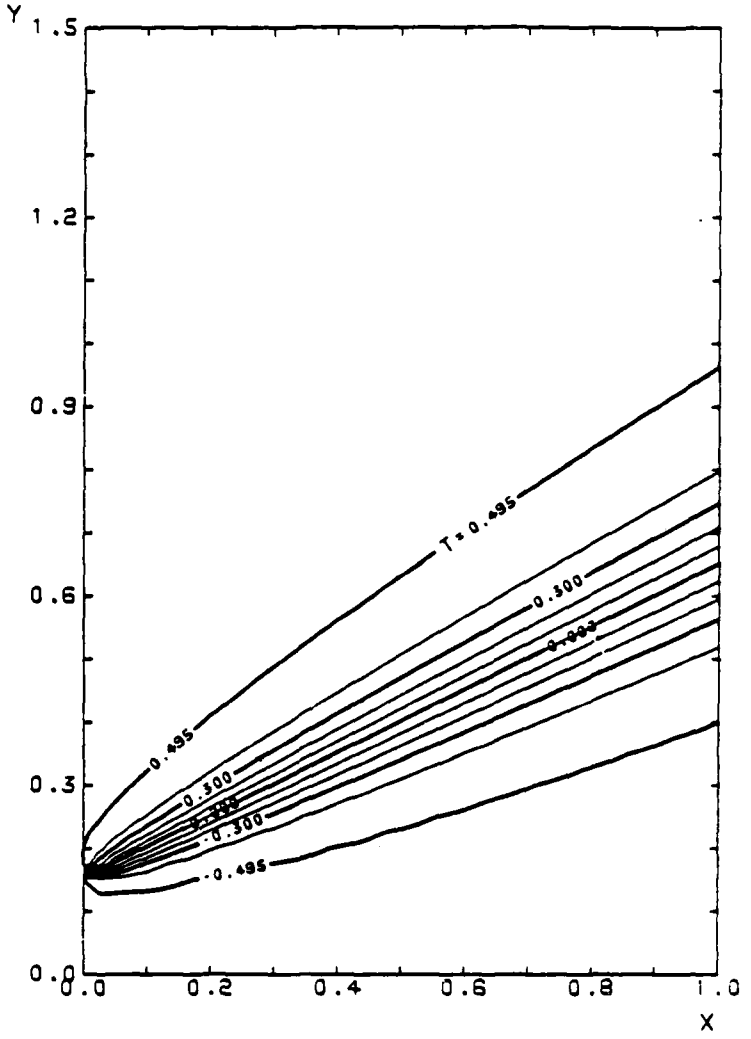

Fig. 10. Numerical solution of a temperature shear layer, grid 120 × 80, no TE injection.

solved on a 60 × 40 base grid of step size $h = 0.25$. A slightly improved solution on an unrotated 120 × 80 grid is shown in Fig. 10 for comparison. This does not compare well with the exact solution depicted in Fig. 11. Given suitable pattern recognition schemes, it would be natural to introduce a rotated grid parallel to the flow direction over a small region surrounding the discontinuity with boundary conditions extracted from the solution in Fig. 9. Here, we have done this manually with a 20 × 40 grid aligned with the flow. Due to grid rotation, the cross-wind artificial diffusion is minimized, resulting in a sharp temperature gradient very close to the exact solution. The isotherms that appear near the upper and lower boundary of the refined local solution on the subgrid (Fig. 12) are an effect of the incorrect boundary conditions extracted from the base grid solution; these can be avoided simply by taking a larger subgrid. However, with the injected TE, the improved base solution provides a

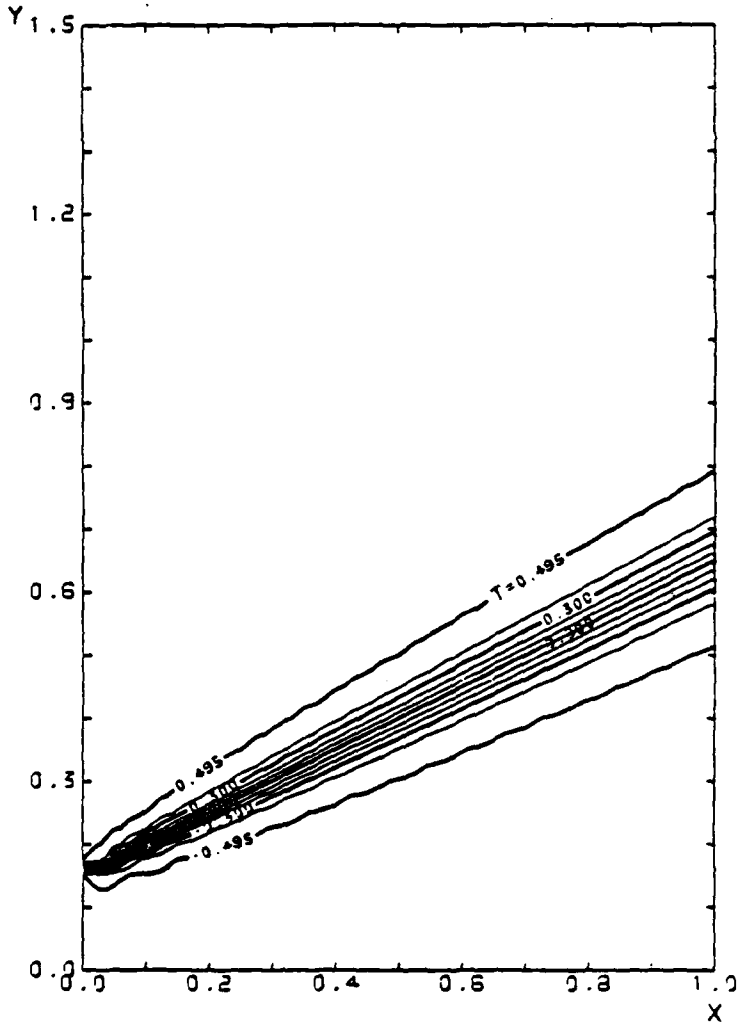

Fig. 11. Exact solution of a temperature shear layer on a grid of 60 × 40.

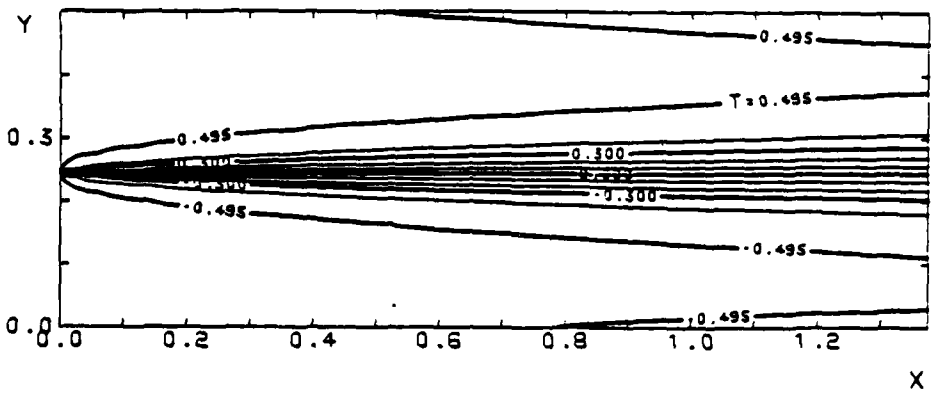

Fig. 12. Locally refined solution on a rotated grid of 20 × 40.

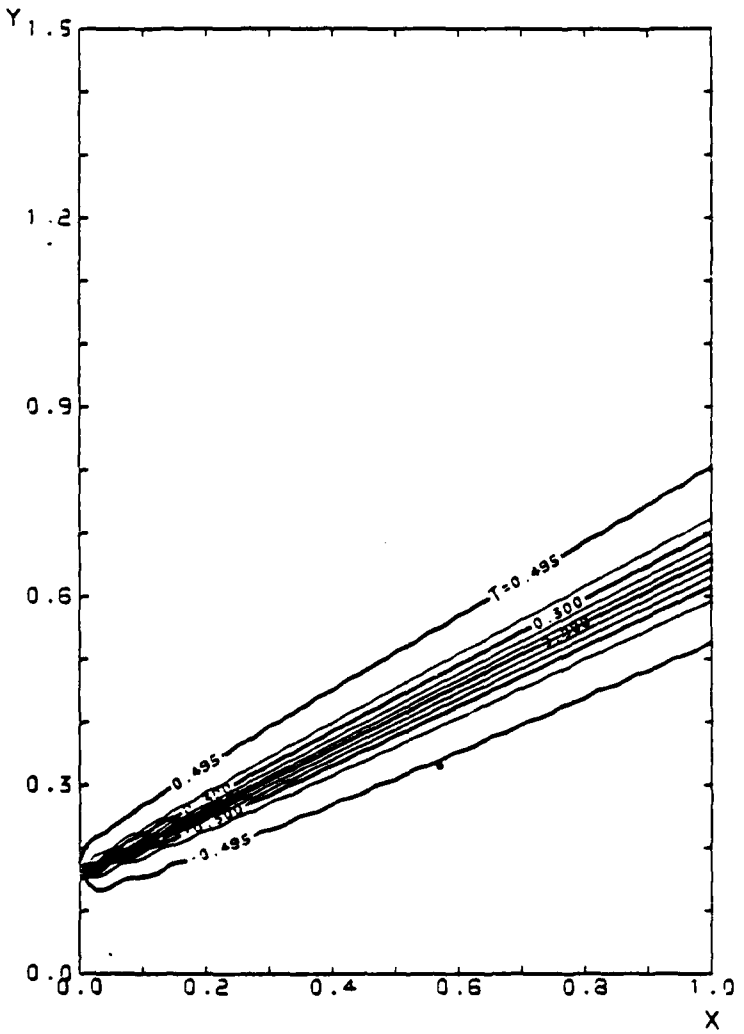

Fig. 13. Improved solution of a temperature shear layer with TE injection, grid 60 × 40.

sharp gradient without such isotherms (Fig. 13), which shows that the base grid solution is readjusted smoothly through the artificial boundaries.

The examples given here demonstrate various aspects of the TE injection method and show, in particular, that very accurate solutions can be obtained on relatively coarse meshes.

5. Conclusions

It is well known that if the truncation error in a discrete approximation to a differential equation were known exactly, the values of the exact solution at the discrete points could be determined. This fact, along with adaptive mesh refinements to determine the truncation error, is used to produce highly accurate solutions to model problems on relatively coarse grids with substantial savings in computer time and use of computer memory. Improvements in the local as well as global accuracy of a solution on a fixed grid are found by refining the grid to estimate the truncation error and by injecting this truncation error back into the solution of the discrete equation on the unrefined grid. This use of solution adaptive grid systems reduces the dependence of the solution on the choice of the grid and, hence, the effort of grid generation.

Acknowledgment

This research was carried out at the Computational Fluid Mechanics Laboratory of the Aerospace and Mechanical Engineering Department under AFOSR Grant 83-0071, monitored by Dr. James D. Wilson, and NASA CFD Traineeship Grant NGT 03-002-800. Permission from Dr. Paul Kutler to use the NASA Ames CRAY-XMP computer for this and other studies related to the traineeship program is gratefully acknowledged. The authors are also indebted to Dr. C.M. Hung of the NASA Ames Research Center for his technical advice.

References

[1] W.C. Thacker, A brief review of techniques for generating irregular computational grids, Internat. J. Numer. Meths. Engrg. 15 (1980) 1335–1341.

[2] J.A. Benek, J.L. Steger and F.C. Dougherty, A flexible grid embedding technique with application to the Euler equations, AIAA Paper 83-1944 (1983).

[3] R. Magnus and H. Yoshihara, Unsteady transonic flows over an airfoil, AIAA J. 13(2) (1975) 1622–1628.

[4] E.H. Atta and J. Vadyal, A grid interfacing zonal algorithm for three-dimensional transonic flows about aircraft configurations, AIAA Paper 82-1017 (1982).

[5] M.M. Rai, A conservative treatment of zonal boundaries for Euler equation calculations, AIAA Paper 84-0164 (1984).

[6] M.J. Berger and J. Oliger, Adaptive mesh refinement for hyperbolic partial differential equations, J. Comput. Phys. 53 (1984) 484–512.

[7] V. Pereyra and E.G. Sewell, Mesh selection for discrete solution of boundary problems in ordinary differential equations, Numer. Math. 23 (1975) 261–268.

[8] G. McNeice and P. Marcal, Optimization of finite element grids based on minimum potential energy, Trans. ASME J. Energy Industry 95(1) (1973) 186–190.

[9] C.E. Pearson, On a differential equation of boundary layer type, J. Math. Phys. 47 (1968) 134–154.

[10] I. Babuška, The self-adaptive approach in the finite element method, in: J.H. Whiteman, ed., The Mathematics of Finite Elements and Applications II. MAFELAP 1975 (Academic Press, New York, 1976).
[11] M. Lentini and V. Pereyra, A variable order finite difference method for nonlinear multipoint boundary value problems, Math. Comput. 28(128) (1974) 981–1003.
[12] R.F. Warming and B.J. Hyett, The modifed equation approach to the stability and accuracy analysis of finite-difference methods, J. Comput. Phys. 14(2) (1974) 159–179.
[13] G.H. Klopfer and D.S. McRae, Nonlinear truncation error analysis of finite difference schemes for the Euler equations, AIAA J. 21(4) (1983) 487–494.
[14] A. Brandt, Multi-level adaptive solutions to boundary value problems, Math. Comput. 31(138) (1977) 333–390.